Defense-related inhibition of sympathetic nerve activity

Insights from neuroimaging and monozygotic twins on related cortical processes and clinical potential

John Jonsson Eskelin

Department of Clinical Neurophysiology
Institute of Neuroscience and Physiology
Sahlgrenska Academy, University of Gothenburg

UNIVERSITY OF GOTHENBURG

Gothenburg 2021

Defense-related inhibition of sympathetic nerve activity:
Insights from neuroimaging and monozygotic twins
on related cortical processes and clinical potential
© Author 2021
john.jonsson.eskelin@gu.se

ISBN 978-91-8009-370-5 (PRINT)
ISBN 978-91-8009-371-2 (PDF)
http://hdl.handle.net/2077/68073

Printed in Borås, Sweden 2021
Printed by Stema Specialtryck AB

Defense-related inhibition of sympathetic nerve activity

Insights from neuroimaging and monozygotic twins on related cortical processes and clinical potential

John Jonsson Eskelin

Department of Clinical Neurophysiology, Institute of Neuroscience and Physiology
Sahlgrenska Academy, University of Gothenburg
Gothenburg, Sweden

ABSTRACT

This thesis investigates a physiological phenomenon observed in the peripheral sympathetic nervous system in response to various stressors and tries to bring it closer to clinical research. Sudden surprising stimulation can evoke a transient inhibition of sympathetic nerve activity to blood vessels in the human body which is also predictive of the blood pressure response. The underlying medical hypothesis is that this may be important for long term blood pressure. In Paper I we investigate the possible genetic contribution to this response pattern in a group of monozygotic twins. Results show that genes do not play a significant role in this response and so the clinical interest is strengthened. In Paper II, correlates to sympathetic inhibition are described in pre-defined areas of the cerebral cortex with magnetoencephalography (MEG) and magnetic resonance imaging. We find strong correlations related to stimulus processing and cortical thickness, as an index of long-term plastic changes. The anterior cingulate, a region known to be involved in threat evaluation and autonomic control, is implicated. In Paper III another of these correlates, namely beta oscillations in the sensorimotor cortex, is used to evaluate the feasibility of using a routine clinical electroencephalogram (EEG) for non-invasive characterization of the peripheral nerve reaction. The prospect of using EEG as a simple mode of classification is not well supported but MEG remains a promising candidate for developing a non-invasive method of gauging individual defense-related responses. Given the role of hypertension as the leading risk factor for global disease burden, a continued evaluation of underlying mechanisms is essential.

Keywords: microneurography, MEG, EEG, MRI, blood pressure, defense reaction, cortical autonomic network

ISBN 978-91-8009-370-5 (PRINT)
ISBN 978-91-8009-371-2 (PDF)

SAMMANFATTNING PÅ SVENSKA

Avhandlingen berör grundvetenskapliga frågor och kliniska tillämpningar rörande det sympatiska nervsystemet, som är avgörande för kontrollen av hjärta och kärl, hos människa. Det har i tidigare studier observerats att kortvariga överraskningsstimuli kan utlösa en dämpning av sympatisk aktivitet till blodkärl i kroppen, i olika utsträckning hos olika individer. Detta samvarierar med reaktiviteten under en mer ihållande kognitiv belastning under flera minuter. Därför kan detta reaktionsmönster tolkas som en del av generaliserade försvarsreaktioner hos människan. I tidigare studier på både djur och människa ser man att blodtryck och nervaktivitet påverkas i samband med försvarsreaktioner, som också kan kopplas till begreppet stress. Stress ökar risken för högt blodtryck och kardiovaskulär sjukdom hos människor. Den underliggande medicinska hypotesen som driver projektet är att individens tendens till att dämpa eller inte dämpa sympatisk aktivitet vid olika former av stress har betydelse för utveckling av kardiovaskulär risk, och därför vore denna tendens intressant att mäta i större skala. Avhandlingen undersöker huruvida 1) det perifera nervsvaret är genetiskt betingat eller föremål för miljömässig påverkan, 2) huruvida det står att finna korrelat till det perifera svaret i hjärnbarkens aktivitet eller struktur, 3) och om ett av dessa korrelat kan utnyttjas som en mer lättillgänglig biomarkör. För den första frågeställningen undersöks en grupp med enäggstvillingar. För den andra frågeställningen används magnetencefalografi och magnetresonanstomografi tillsammans med nervregistreringar och blodtrycksmätningar och följs upp med elektro-encefalografi, för den tredje frågeställningen. Elektroencefalografi är en metod som används i klinisk rutin på sjukhus världen över. Resultaten visar att det finns en koppling mellan sensori-motoriska delar och andra delar av hjärnan som är involverade i reglering av cirkulation och utvärdering av yttre miljö och de svar som kan mätas i nerver och blodkärl i kroppens periferi. Utsikterna att använda elektroencefalografi är mindre övertygande. Resultaten bör utforskas vidare med hjälp av kombinerade metoder för nervregistrering och neuroimaging i syfte att förstå fenomenet med sympatisk inhibition bättre, samt att förenkla proceduren med att karaktärisera svarsprofiler jämfört med krävande nervregistreringar. På så vis kan de oklarheter som fortfarande omger uppkomsten av högt blodtryck komma att förstås bättre.

LIST OF PAPERS

This thesis is based on the following studies.

I. Lundblad, L. C., Eskelin, J. J., Karlsson, T., Wallin, B. G., & Elam, M.

Sympathetic Nerve Activity in Monozygotic Twins: Identical at Rest but Not During Arousal. *Hypertension* 2017; 69(5): 964-969.

II. Riaz, B., Eskelin, J. J., Lundblad, L. C., Wallin, B. G., Karlsson, T., Starck, G., Lundqvist, D., Ooostenveld, R., Schneiderman, J. F., & Elam, M.

Brain structural and functional correlates to defense-related inhibition of muscle sympathetic nerve activity in man. *Manuscript*.

III. Eskelin, J. J., Lundblad, L. C., Wallin, B. G., Karlsson, T., Riaz B., Lundqvist, D., Schneiderman, J. F., & Elam, M.

Simultaneous recordings of EEG and MSNA during somatosensory stimulation – prospects of a non-invasive biomarker for defense-related sympathetic inhibition. *Manuscript*.

CONTENT

ABBREVIATIONS

Ag/AgCl	Silver, Silver Chloride
ANS	Autonomic Nervous System
AUC	Area Under the Curve
BA	Brodmann Area
BF	Burst Frequency
BI	Burst Incidence
BP	Blood Pressure
BRR	Baroreceptor Reflex
CAN	Central Autonomic Network
CVLM	Caudal Ventrolateral Medulla
DBP	Diastolic Blood Pressure
ECG	Electrocardiogram
FWHM	Full Width Half Maximum
GABA	Gamma-Aminobutyric Acid
GSR	Galvanic Skin Response
ICA	Independent Component Analysis
MAP	Mean Arterial Pressure
MEG	Magnetoencephalography
MNG	Microneurography
MRI	Magnetic Resonance Imaging

MSNA	Muscle Sympathetic Nerve Activity
NE	Nor-Epinephrine
NTS	Nucleus Tractus Solitarius
PAG	Periaqueductal Grey area
ROI	Region of Interest
RVLM	Rostral ventrolateral medulla
SBP	Systolic Blood Pressure
SNA	Sympathetic Nerve Activity
SNS	Sympathetic Nervous System
SPM	Statistical Parametric Mapping
SQUID	Super-Conducting Quantum Interference Device
SSNA	Skin Sympathetic Nerve Activity
TE	Echo Time
TR	Repetition Time

1 INTRODUCTION

This introduction begins with an overview of the organization of the sympathetic nervous system and cognitive processes affecting circulatory control are highlighted. Then follows an account of how to measure muscle sympathetic nerve activity (MSNA) in humans. MSNA is central to the work in this thesis. 'Defense-related inhibition of sympathetic nerve activity' is then reviewed, which forms the basis for the analysis of all the neuroimaging indices, which are also explained. A clinical outlook towards hypertension and cardiovascular risk is also included.

1.1 The sympathetic nervous system

The circulatory system evolved out of necessity to effectively provide oxygen and nutrients to all parts of the organism. Because its role is so essential, the basic functions are largely automated and the structure is relatively conserved across mammalian species. The functions of the circulatory system enable constant adaptation to almost everything that we do in our daily lives. Neural control of circulation is relegated to the branch of the nervous system called the autonomic nervous system (ANS), meaning self-governing. The ANS is divided into the sympathetic (SNS) and parasympathetic nervous system). The subdivision primarily responsible for blood pressure regulation is the sympathetic branch (i.e., the SNS). The ANS is often thought of as beyond voluntary control, but it is clear, however, that many pathways exist that allow human beings to consciously tap in to the control of this system.

1.1.1 Brain nuclei and pathways

The SNS is organized into nuclei containing premotor neurons in the brainstem that project onto pre-ganglionic neurons in the spinal cord and onto post-ganglionic neurons outside the spinal cord, as well as a central autonomic network (CAN) including cortical regions modulating the central nuclei. The premotor neurons are located in the ventral lateral part of the medulla oblongata in the brainstem. A rostral and a caudal section have been identified (RVLM and CVLM) of which the RVLM is predominantly excitatory and CVLM contain neurons that inhibit the RVLM (Schreihofer and Guyenet, 2002). Classification of catecholaminergic cell populations have resulted in A-class and C-class neurons (Dahlstroem and Fuxe, 1964). Adrenergic C1 neurons make up much of RVLM: 2/3 are adrenergic and others are glutamatergic (Jänig, 2006). C1 neurons are important for acute stress, (Guyenet et al., 2001) and the RVLM seems to relay activity to several, if not

all, sympathetic branches to the heart, kidneys, adrenal glands and blood vessels in the gut, as well as skin and muscle tissues; there is furthermore evidence of a roughly topographic organization (McAllen and Malpas, 1997). These premotor neurons communicate with other nuclei in the brainstem and several cortical regions (cf below).

From the brainstem, axons of premotor neurons pass downward in the spinal medulla before synapsing on to pre-ganglionic neurons in the lateral horn of the spinal cord. Pre-ganglionic axons then project to the sympathetic ganglia, which are collections of nerve cell bodies resting just lateral to the spinal cord. These synapses are cholinergic at this stage (acetyl-choline as neurotransmitter) and the axons of the post-ganglionic neurons carry the signal to the intended target, e.g., the smooth muscle cells surrounding blood vessels. Post-ganglionic cells release the neurotransmitter norepinephrine (NE) on alfa or beta receptor types on the target cells leading to activation. Efferent activity to sweat glands is an exception to this rule, though, as these synapses remain cholinergic. The adrenal glands, which release epinephrine, are also a special case because they are themselves transformed postganglionic neurons and are thus activated by cholinergic preganglionic neurons directly. The nerve fibers (axons) of the sympathetic nervous system belong to the group of unmyelinated slowly conducting C-fibers. These have an approximate conduction velocity of 0.5-2m/s. A peripheral nerve consists of several fascicles (fiber bundles) and the sympathetic fibers run in the very middle of each nerve fascicle, supported by Schwann cells. The above details are specific to the efferent fibers (outgoing traffic). Afferent nerve fibers (ingoing traffic) are poorly studied and are called visceral afferents without sympathetic and parasympathetic classification.

The RVLM generates excitatory activity to different parts of the sympathetic system, but the behavior of sympathetic activity to skin is different from that to muscle, and both differ from that to kidneys (Jänig and Häbler, 2003; McAllen and Malpas, 1997). The most pertinent example is the connection between parts of sympathetic nerve activity (SNA) to the baroreceptor-reflex (BRR) (Schreihofer and Guyenet, 2002). SNA to blood vessels constricts the vessels which increases vascular resistance and raises blood pressure (BP). For BP to remain stable, as BP drops SNA should increase and when BP is too high SNA should be inhibited. This is accomplished through barosensitive neurons in the carotid bodies of the neck and aorta which sense arterial BP fluctuations with each heart beat and respond immediately with signals to the nucleus tractus solitarius (NTS) further onto the CVLM, inhibiting the RVLM (Dampney, 1994) as illustrated in figure 1.

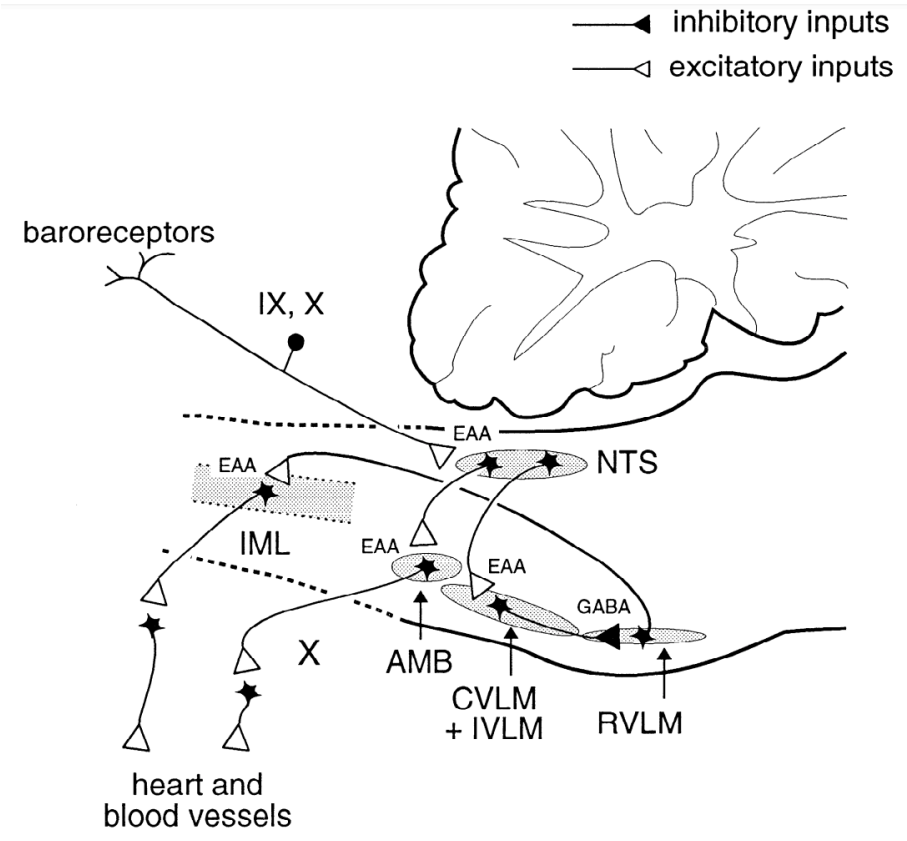

Figure 1. The suggested brainstem nuclei and connections involved in the baroreceptor reflex. NTS: nucleus tractus solitarius; CVLM: caudal ventrolateral medulla; IVLM: intermediate VLM; RVLM: rostral VLM; IML: intermediolateral column; IX: glossopharyngeal nerve; X: vagus nerve; AMB: nucleus ambiguus; EAA: excitatory amino acids; GABA: gamma-amino-butyric acid. (Adapted by permission from: Dampney RA. (1994). Functional organization of central pathways regulating the cardiovascular system. Physiol Rev, 74:323–364.).

1.1.2 Central autonomic network

Apart from the basic functions of nuclei in the brainstem discussed above, there are other structures in the brain that interact with these cell groups and the circulatory system. The amygdala is central to fear and anxiety and defensive behavioral patterns (LeDoux and Daw, 2018). The hypothalamus is a group of nuclei at the heart of homeostatic endocrine regulation including cortisol levels and also defense reactions to threat and stressors (DiMicco et al., 1996). There are also two main cortical regions that, together with the deeper structures,

form a central autonomic network (CAN, see figure 2). These cortical regions are the Insula and the Cingulate cortex (Benarroch, 2012).

Higher-level cognitive functions associated with the cerebral cortex may give rise to feelings of anxiety, fear, anger for example that are also accompanied by autonomic reactions. The triggers can rely on memories or arise as a result of complex stimuli that often require integration of contextual information. Both the insula and cingulate cortex are transitional zones between the phylogenetically old parts of the brain and the more recently evolved neocortex. The Insula has been described as being important for interoceptive awareness and the emotional state as well as cardiovascular control (Craig, 2002; Oppenheimer et al., 1992). The cingulate is a very diverse region, and while it is tempting to attribute one clear purpose to a particular area it is implicated in a myriad of different contexts related to autonomic control, memory, evaluation, decision making, reward, emotions, defensive behavior, and several others (Critchley et al., 2011; LeDoux and Daw, 2018; Roy et al., 2012). It is however undeniably linked to autonomic regulation.

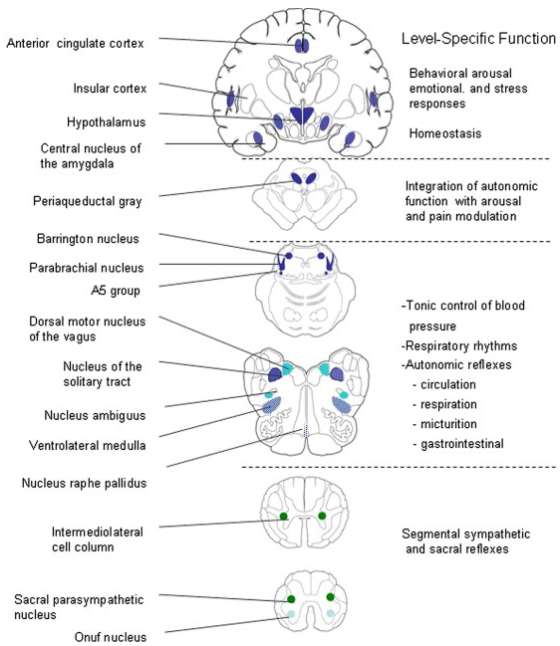

Figure 2. The central autonomic network. (Reprinted from: Primer on the Autonomic Nervous System (Third Edition): Central Autonomic Control. Benarroch EE, eds Robertson, D, Biaggioni, I, Burnstock, G, Low, PA, Paton, JFR,. pp 9–12. Copyright, 2012, with permission from Elsevier.)

1.2 Measuring sympathetic activity

1.2.1 Microneurography

In research on the sympathetic nervous system in humans, microneurography (MNG) has ever since its birth in Uppsala in the 1960s been considered the 'gold standard' (Hagbarth and Vallbo, 1968; Shoemaker et al., 2018). With this method it is possible to record action potentials from single neurons in the human body. The human autonomic nerve fibers readily available to a researcher are 1) efferents to blood vessels in skin and 2) muscle and 3) those to sweat glands (all belonging to the SNS).

The initial steps in microneurography towards establishing the recording site is to palpate the location of the nerve, then with a blunt surface electrode roughly the size of a small pencil, stimulate the nerve non-invasively and mark potential points of entry on the skin with a pen. The locations are marked based on muscular contractions and skin sensations of the innervated area of the lower extremity in the subject. Then a differential pre-amplifier is attached close to the recording site and two tungsten microelectrodes are inserted under the skin: a non-insulated low-impedance reference electrode in the dermis layer, and an insulated high-impedance electrode through the dermis at one of the target locations (figure 3). This is followed by the administration of repeated test pulses of electrical stimulations through the needle electrode at 1-3 V, while the electrode is maneuvered closer and closer to a nerve fascicle of interest. The needles are 2-4 micrometers wide at the tip, and are blunt-tipped so as to avoid any damage to the nerve. Once the perineurium is reached and penetrated, the stimulation is turned off and the investigator adjusts the electrode position inside the impaled fascicle while viewing and listening to the signal. Each fascicle contains a mix of different nerve fibers so the experimenter must differentiate between muscle afference, skin afference, sympathetic skin efference destined for sweat glands and blood vessels (SSNA), and sympathetic muscle efference to blood vessels (MSNA). When searching for sympathetic activity this is done through manipulation of the extremity and sympathetic outflow through the use of maneuvers (Vallbo et al., 1979). The time to establish a successful recording site varies widely from 0.1 – 2.5 hrs with a median time of about 1 hr. Once a site has been found, the subject must remain quite still to avoid losing the recording site. Because the fascicle has a diameter of only about 1mm, even slight movement may cause the electrode to slip out of the nerve fascicle, forcing a restart of the procedure if it is not abandoned altogether.

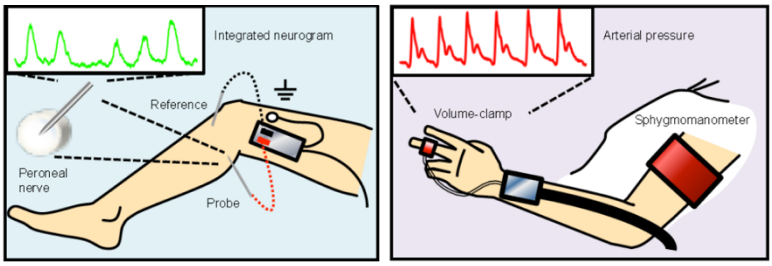

Figure 3. Schematic illustration of the microneurography setup and concomitant blood pressure measurements used in the experiments.

It should also be mentioned that, when microneurography is not feasible, measuring the plasma NE released from nerve terminals through catheterization and repeated blood sampling provides a time-integrated estimation of sympathetic activity enabled through an isotope dilution method (Esler et al., 1988). For example, the kidneys and the heart receive sympathetic innervation but the nerves are inaccessible. These nerves influence the rate and contractility of the heart, and the glomerular filtration rate in the kidneys and thus fluid balance and osmolality in the blood. The latter contributes to regulating blood pressure on a slower timescale (Guyton et al., 1969) while the heart and MSNA typically operate on a moment to moment basis.

1.2.2 MSNA

MSNA is heavily influenced by the physiological negative feedback loop called the baroreceptor reflex, as are the kidneys but activity to skin is almost entirely disconnected from it (Fagius et al., 1985). Therefore, it is tightly coupled to blood pressure fluctuations, while skin is not (Delius et al., 1972a; Wallin, 2006; Wallin and Elam, 1997). In normal circumstances the MSNA is organized in bursts, and each burst is tied to a particular preceding cardiac interval. Each burst is made up of vasoconstricting nerve impulses which serve to raise vascular resistance and BP. The incidence of bursts is governed by a central drive and is modulated by the BRR. (Fagius et al., 1985). Because the bursts are generated in the central nervous system and the activity is recorded in the periphery there will also be a latency related to body height and length of the extremity that needs to be accounted for (about 1.2 - 1.5 s at the common peroneal nerve) (Fagius and Wallin, 1980; Sundlöf and Wallin, 1978; Wallin and Rea, 1988). Sympathetic activity is either recorded and analysed as single unit action potentials or as groups of action potentials (multiunit activity) commonly referred to as bursts. It is common to use these modes separately as the recording of single action potentials require a much greater sampling frequency and therefore greater digital storage capacity and processing power

of the equipment. Bursts are often displayed as a rectified signal (root-mean-square) to facilitate the identification of peak amplitude, duration and latency.

In the resting state, these bursts can be quantified as either bursts per minute (burst frequency, BF) or bursts per one hundred heartbeats (burst incidence, BI). BI is used most often as a way to describe the general set point for activity in an individual, whereas BF can be better applied as a measure of exposure, such as in correlations to cardiovascular risk during a lifetime as it correlates stronger to levels of norepinephrine in blood samples (Wallin, 1988). MSNA at rest is a stable characteristic in a person which is strongly influenced by genetics as shown by recordings from monozygotic twins, but it tends to increase with age (Ng et al., 1993; Sundlöf and Wallin, 1978; Wallin et al., 1993). The activity is believed to be mirrored in all the skeletal muscle tissue of the body as shown by simultaneous recordings in the arm and leg both at rest and during provocations (Carter et al., 2005; Cui et al., 2015; Wallin and Rea, 1988). As a need for more vasoconstriction occurs it is first accomplished through increased burst incidence, then increased amplitude through recruitment of more fibers, and as a further mechanism the firing rate of individual fibers is increased (Elam and Macefield, 2001; Macefield et al., 1999; Macefield and Wallin, 2018). MSNA may be further influenced by recent food intake, BMI, temperature, hydration level, mental state and biological sex (Fagius, 2003; Low et al., 2011; Posch et al., 2017; Robinson et al., 2019; Scalco et al., 2009; Tank et al., 2008).

Experimental models investigating the dynamics of MSNA have focused much on stress in various forms. Cognitive load is known to affect MSNA with varying outcomes in different individuals (Carter and Ray, 2009; Donadio et al., 2012; El Sayed et al., 2018). Another method for modulation is the cold-pressor test, wherein a painful stimulus is induced by submerging the hand in ice-water (Victor et al., 1987). Static handgrip, as a model of physical exercise/effort, also leads to increased levels of MSNA (Mark et al., 1985). Cognitive stress models often produce conflicting results though, which may depend on interactions with the blood pressure response and its feedback through the baroreceptor reflex. But a recent assessment reported good test-retest repeatability (Fonkoue and Carter, 2015).

Much time and effort has been devoted to the study of the relationship between sympathetic activity and blood pressure in humans, not least in the field of hypertension research. For this particular problem, kidneys and skeletal muscle tissue may be regarded as the most important. Skeletal muscle tissue contains a significant volume of blood. With a change in blood vessel diameter it should

therefore have a large impact on systemic vascular resistance and blood pressure.

Studies show a statistically significant relationship between the amount of sympathetic nerve activity and hypertension and cardiovascular risk (Grassi et al., 2018; Yamada et al., 1989). However, the circulatory system is highly complex and many interactions and compensatory mechanisms exist (e.g. endocrine, paracrine, neural, behavioral, transduction) which may complicate correlations between MSNA and BP. Probably as a result of this multifactorial system the inter-individual variability of resting levels of MSNA is large. This also means that the predictive value for hypertension (cf ch 1.3) on an individual level is practically non-existent.

1.2.3 Defense-related inhibition

The sympathetic nervous system has always been a focus of those interested in stress and so-called defense reactions. In animal experiments central nervous system structures common to several mammal species have been identified. The hypothalamic defense area, the dorsomedial hypothalamus, the paraventricular nucleus, PAG and amygdala are all important for defensive reactions in response to various stressors (Dampney et al., 2013; Dampney et al., 2018; DiMicco et al., 1996; Fontes et al., 2011; LeDoux and Daw, 2018). Integrative models of cardiovascular and behavioral patterns in response to stressors describe several phases of a cascading series of reactions beginning with the stage called arousal (Kozlowska et al., 2015). This is a state of heightened vigilance in preparation for action which may then progress to e.g. a fight-or-flight or a freezing type response which all require that the circulatory system adapts to the new set of circumstances.

The MSNA reaction to arousal has been characterized in humans by introducing unexpected events of visual, auditory or somatosensory stimulation. An inhibitory response is normally seen for up to two cardiac intervals immediately following stimulation (Donadio et al., 2002a; Donadio et al., 2002b; Lundblad et al., 2017). Such inhibition is only apparent in some individuals however, and repeated examination has shown this tendency to be reproducible. MSNA inhibition is furthermore coupled to blood pressure reactivity such that it is related to attenuation of the blood pressure increase otherwise seen in response to the stressors, shown in figure 4 (Donadio et al., 2002b). Furthermore, one study has shown a negative correlation between the degree of arousal induced inhibition and change in MSNA during mental stress, see figure 4 (Donadio et al., 2012). This suggests that the underlying reactions to both sudden and longer lasting stressors are related. However,

submerging the hand in ice-water as a form of pain stimulus did not show the same correlation, revealing also a specificity for certain types of stressors. Another point of evidence towards a cognitive or cortical coupling to defense related inhibition of MSNA is the observation that patients with phobia induced syncope (phobic fainting) displayed a prolonged inhibition of MSNA to sudden stimuli (Donadio et al., 2007). This was not present in normal controls nor in syncopating patients lacking a phobic component. In summary, MSNA inhibition may be a marker of a generalized trait for modulation of circulatory changes during various forms of stress which may be of further clinical interest.

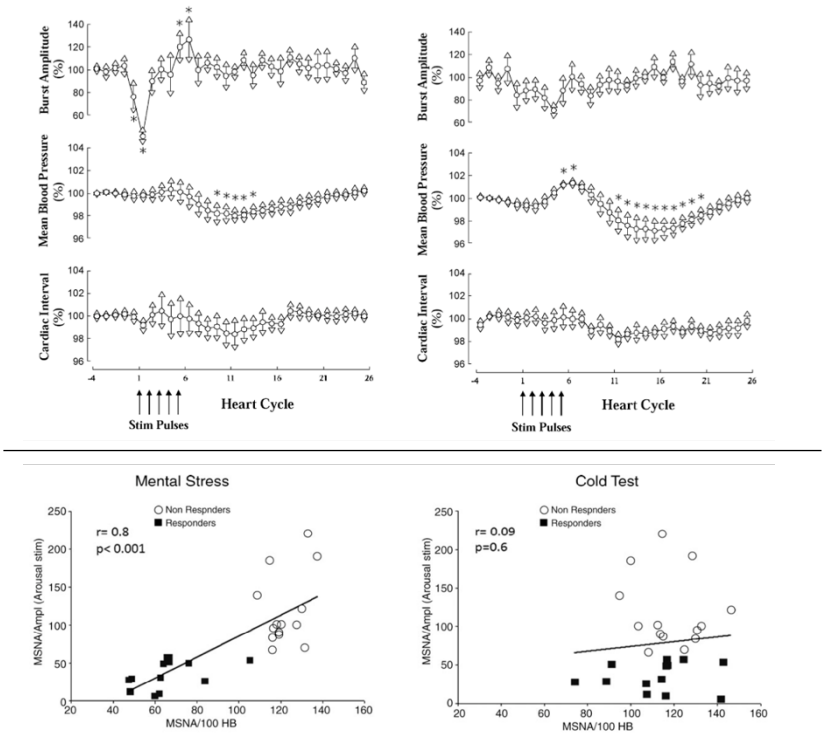

Figure 4. Top: Changes induced by arousing electrical stimulation in MSNA, mean BP and heart rate in subjects with and without significant MSNA inhibition. (Reprinted by permission from: Donadio V, et al. (2002b). Interindividual differences in sympathetic and effector responses to arousal in humans. J Physiol, 544:293–302.). Bottom: Correlation between change in MSNA during arousing stimulation and i) 3 min of mental stress or ii) cold pressor test. (Adapted by permission from Donadio V, et al. (2012). Muscle sympathetic response to arousal predicts neurovascular reactivity during mental stress. J Physiol, 590:2885–2896.).

1.3 Blood pressure and cardiovascular risk

When a person's BP level is manifestly elevated above 140/90 mmHg it is called hypertension (recently updated recommendations: 130/80 mmHg, (Whelton Paul K. et al., 2018)). This is associated with increased risk for cardiovascular disease in the long term and is considered to be one of the top independent factors of global disease burden in the world (Lim et al., 2012; NCD-RisC, 2017). Many cases of hypertension are diagnosed without an apparent cause or is mainly attributed to lifestyle factors, called *essential*, or *primary*, hypertension. The emergence of hypertension in an individual is multifactorial, and much remains to be understood. However, the neural regulation is believed to be an important player in initiating a development towards a pathological increase in BP level, and repeated exposure to stress may be particularly important (Korner, 2007). Not only BP level but also BP variability between repeated measurements and BP reactivity to stressors have been associated with increased risks (Chida and Steptoe, 2010; Stevens et al., 2016).

It has been shown in a highly controlled study that moving from a rural area into an urban environment leads to increased BP levels, strongly indicating that increased stress is a major factor (Hollenberg et al., 1997). Furthermore, a 30 year follow up compared nuns living in a secluded order in northern Italy to a group of lay women from the neighboring area (Timio et al., 1988; Timio et al., 1997; Timio et al., 1999). Significant blood pressure differences were observed, again suggesting that the environment and the stress it brings is important. This was a gradual process over many years before the differences emerged. Thus, long term exposure to environmental stressors is likely the first step on a downhill path that is known to lead to permanent structural alterations in the vascular system and organ deterioration as a consequence of increased vascular resistance over time. However, in spite of much research in both humans and animals it is not always clear why hypertension develops, and the role of the SNS as well as that of gene-environment interactions is still debated (Esler, 2011; Guyenet, 2006; Korner, 2007).

The clinical relevance of this thesis rests on the proposition that defense-related inhibition of MSNA reflects an individual propensity towards specific reaction patterns that may be a risk factor of hypertension in the long run. This is worth pursuing to understand the possible risks involved and how to counter such a development for the sake of long-term health. Thus far, no study has looked into related brain processes, and doing so could produce tools to facilitate studies in larger populations.

1.4 Brain imaging

1.4.1 Magnetic resonance imaging

Magnetic resonance imaging (MRI) is widely used in both clinical routine and research and can include both functional and structural sequencing of the brain. Aside from morphometry of the brain with a common T1/T2/PDI protocol, various other structural modes of acquisition exist such as tractography, SWI, DWI, T2-flair which are used for specialized inquiries into brain morphology and pathology. Common T1 weighted images however are optimized for good contrast between grey and white matter in the brain. The ability to distinguish grey matter from other tissue can then be exploited to non-invasively gauge e.g. integrity of the neuronal populations in the cerebral cortex after isolated lesions (Abela et al., 2015), patterns of atrophy as in Alzheimer's disease (Baron et al., 2001) and plastic changes as a result of learning (Amunts et al., 1997; Maguire et al., 2000; Sluming et al., 2002).

Scans from MRI are essentially grayscale images in 3 dimensions. Various software packages are available for analysis of such image volumes. The first principle developed was voxel-based morphometry (VBM, voxel is a 3D pixel) using statistical parametric mapping (SPM), a method available in the widely used SPM series of software (Ashburner and Friston, 2000). This is based on measuring voxel intensities in 3D space and segmenting the image into grey and white matter for further statistical comparisons. In more recent times, another approach has been developed which uses a surface-based approach for cortical reconstruction available in the also popular FreeSurfer package (Dale et al., 1999; Fischl et al., 1999) and has been histologically validated (Cardinale et al., 2014). The main differences between these two fundamentally different ways to classify grey and white matter in the brain can be said to lie in the effects of image smoothing and the scope of applications. VBM measures image intensity in each voxel and compares this to a tissue probability map before deciding on the tissue identity of the specific voxel. This can be applied to the whole brain, including subcortical volumes e.g. brainstem, diencephalon and cerebellum. FreeSurfer on the other hand, reconstructs the folded structure of the cortex into a 2-dimensional surface coordinate system based on individual gyral folds. The surface map is then inflated to a sphere, before co-registration to a common template brain (if a template is used). Then parameters such as curvature or thickness in each vertex can be computed and compared between individual brains in a shared coordinate system. The results for SPM and FreeSurfer respectively are then expressed either as grey matter volume (or sometimes concentration) or cortical thickness. The surface-based reconstruction method can only be applied to the cerebral cortex (while in

theory also the cerebellar cortex, the technical difficulties have not yet been overcome).

Both methods require smoothing of the images in order to improve alignment and to increase statistical power. An advantage for FreeSurfer is often said to be the fact that the necessary smoothing step occurs on a 2-dimensional map in which the gyri have first been separated some distance apart, rather than in the original 3D space, thus avoiding undesirable interactions of voxel intensities across gyri. Furthermore, thickness measures are independent of total intracranial volume i.e brain size, in contrast to volume-based measures.

1.4.2 Electrophysiological imaging

The brain can also be examined with regards to the activity generated within. While direct recordings of neuronal activity in humans are limited to neurosurgical procedures, brain function can be assessed non-invasively by measuring at the scalp. The cortical surface is organized in cellular layers and the pyramidal layer contains so-called pyramidal neurons, named after the shape of the cellular soma (cell body). Neurons are connected through synapses which can be inhibitory or excitatory as they induce negative or positive ionic currents flowing in and out of the cell. These currents across the membrane also give rise to secondary currents along the cellular membrane of dendrites and axons through a sink-source dynamic (Lopes da Silva, 2010).

These neurons are furthermore organized in parallel columns. Due to this columnar organization the currents generated by synaptic potentials along the axons tend to sum up and thus give rise to measurable magnetic and electric fields at the scalp. This neural activity from a set of cortical columns can be modeled as an equivalent current dipole, containing a location, direction and magnitude (arrows, figure 5).

1.4.3 Magnetoencephalography

From physics we learn that an electric current generates a magnetic field that circles around and perpendicular to the current according to the right-hand rule. Magnetic fields caused by a minimum of a 10 nAm current can be measured with magnetoencephalography (MEG), and corresponds to the summated excitatory post synaptic potentials from ~50000 synchronously active neurons. This corresponds to the area of a circle with a diameter of about 1 mm. Due to the behavior of magnetic fields, MEG systems are most sensitive to cortical current dipoles that are tangential to the scalp; radial sources (i.e., pointing directly out of the head) produce vanishingly small magnetic fields outside of the head (Lopes da Silva, 2010)(cf. figure 5).

A MEG-system is made up of a sensor array of superconducting quantum interference devices (SQUIDs) in the shape of a helmet, that can contain over 300 sensors. Above the array is a dewar filled with a cryogenic liquid (e.g. helium), cooling the sensors to a temperature as low as 4° K (–270° C) which is necessary for the superconducting properties to emerge. Field strengths from the brain are on the order of 10^{-15} T whereas the Earth's magnetic field is about eight orders of magnitude stronger. This, and other sources of magnetic fields (e.g., cars, electronics, elevators, etc.), cause considerable noise which therefore requires that MEG be recorded in specially designed magnetically shielded rooms. The sensors come in different configurations. Magnetometers use a single pickup loop which makes them best at detecting source fields (unit tesla, T) some distance away from the sensor, but also vulnerable to parallel fields from background noise. Gradiometers are designed to cancel background noise from parallel fields by using two intertwined pickup loops which thus measure a field gradient instead (T/m) - axial gradiometers have loops in two planes, and planar gradiometers have the loops in the same plane. In contrast to magnetometers, gradiometers have greater sensitivity for sources located near the sensor (Parkkonen, 2010).

A MEG sensor array is thus a complicated setup that requires much computational power and knowledge of the signal to process and interpret. This complexity, however, in combination with the low distortion from neighboring tissue is what allows powerful spatial localization of the underlying neural sources. Because of the indirect and ambiguous nature of the signal, however, there is not a single unique solution for where the activity was generated. This is called the inverse problem and is solved by the choice of a computational model built around some specific constraints.

Source reconstruction consists of constructing a leadfield (a model of the coupling between the sensors in the MEG system and the set of neural sources, generated from a subject-specific MRI of the brain) and then selecting a section of MEG-data and calculating the most probable source of this data. The most common methods of source reconstruction are the dipole method, the beamformer method, or minimum norm estimates. These are all very different principles. The dipole model is heavily constrained as the signal is only allowed to be in the form of one or a few dipoles, which may be suitable for well-known and well-defined activity. Distributed source models like beamformers and mininum-norm estimates, on the other hand, do not rely on such constraints and, instead, generate an estimate of the activity of thousands of sources in the brain.

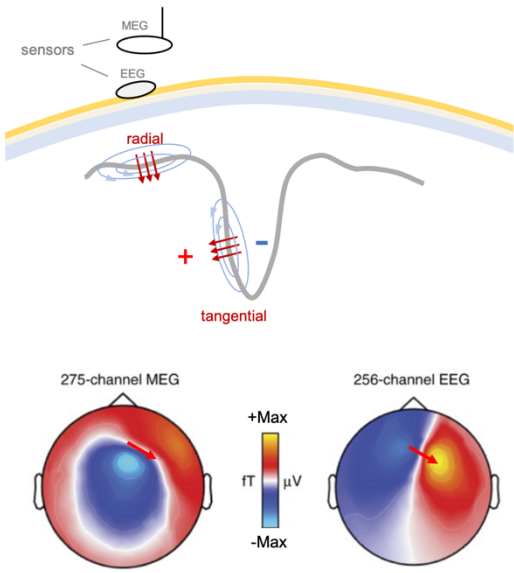

Figure 5. Top: EEG and MEG measure the fields from electric volume currents and magnetic fields generated from the neuronal primary currents, respectively. MEG sensitivity is poor for radial sources. Bottom: Differences in the field topography in MEG and EEG generated from the same dipole source (Adapted by permission from: Baillet, S. Magnetoencephalography for brain electrophysiology and imaging. Nat Neurosci 20, 327–339 (2017)).

1.4.4 Electroencephalography

As an alternative to the complicated task of setting up and making sense of the magnetic fields, one may also choose to characterize the workings of the neuronal signaling from electrical potentials that propagate through the skull. The ionic currents created by cortical columns are oriented radially to the cortex (in contrast to the perpendicular magnetic fields) and so has greater sensitivity for gyral folds close to the surface i.e., electroencephalography (EEG) is sensitive to so-called radial sources to which MEG is relatively insensitive. These currents are affected by the conductivity (dielectric properties) of each medium in the cranial volume as they propagate first through brain tissue, the cerebrospinal fluid, meninges, the skull, and skin before reaching an electrode at the scalp. This is called volume conduction and causes the signal to be smeared out, in contrast to magnetic fields that are relatively unaffected by tissue conductivity (Lopes da Silva, 2010; Muthukumaraswamy, 2013). This is also what makes EEG so sensitive to noise

originating in muscle tissue (Goncharova et al., 2003; Keren et al., 2010; Whitham et al., 2007; Whitham et al., 2008). Muscle contraction is caused by depolarization of skeletal muscle cells. Because those currents are not impeded by the skull and other interfaces before reaching the electrodes, their electric potentials are significantly stronger than, and tend to overpower, those generated by neural sources.

EEG electrodes are always relative to a point of reference, either a dedicated electrode or calculated from a combination of electrodes, and the choice of reference will impact the signal and interpretation (Yao et al., 2005; Yao et al., 2019). Because of volume conduction source localization is much less precise and favors a large number of channels (Ding and Yuan, 2013; Puce and Hämäläinen, 2017). An advantage of EEG is its practical simplicity; it has been around for almost a hundred years (Gloor, 1969) and there is no need for expensive infrastructure. EEG and MEG can complement each other through their differences, and they share the origin of the signal and a great temporal resolution on the ms level.

1.4.5 Neural oscillations

One way to analyze activity from EEG and MEG is to characterize the presence of oscillations. Neural oscillations have been described since the beginning of EEG and are divided into several canonical bands; Alpha, Beta, Delta, Gamma, Theta. They all have different physiological connotations. Alpha rhythms dominate in the occipital cortex as a resting rhythm due to reciprocal connections to the thalamus, and emerges most fully when eyes are closed. Beta rhythms are found all over the cortex and have different meanings depending on location, but may in general be used as a hallmark of the conscious state. Normally, Theta and Delta emerge during sleep. Slightly varying definitions of these frequency bands exist as e.g. beta may be said to include both 12-30 or 13-30 Hz, and ambiguity sometimes surrounds the frequencies at the transition from one band to another.

The amplitude of neural oscillations is proportional to the level of synchronous activity from a large population of cells, although this is an interpretation and not a fact. A decrease in amplitude (oscillatory power) suggests that neural activity is desynchronized which is generally considered to mean an active state. Conversely, an increase in amplitude suggests the neuronal populations are synchronized, which can be a sign of a resting state or inhibitory rhythm. Alternatively, it may be a sign of reciprocal communication over a distance – the idea being that the longer the distance, the lower the frequency of the

oscillations due to the inherent conduction latencies involved (Engel and Fries, 2010; Kilavik et al., 2013).

In relation to somatosensory stimulation (similar to what was used in previous studies of arousal-induced sympathetic inhibition, ch 1.2.3) a response in the beta band is known to occur in the sensorimotor cortex. Typically, a period of desynchronization followed by resynchronization is seen (Cheyne, 2013; Salenius et al., 1997).

2 AIM

i) To probe the clinical potential of the MSNA response to transient stimuli by investigating the possible genetic influence on defense-related sympathetic inhibition.

ii) To investigate the possible presence of functional and structural correlates in the cerebral cortex to MSNA inhibition in the hopes of finding a non-invasive marker of the response.

iii) Evaluate the potential of a non-invasive surrogate to invasive microneurography recordings using a clinically accessible method.

3 METHODS

3.1 Participants

In study one 10 pairs of monozygotic twins were recruited from the Swedish National Twin registry upheld by Karolinska Institute. In study two and three, participants were recruited from local university notice boards at medical and technological faculties. Participants were of ages 18-45 and of male gender and exclusion criteria were any condition or substance use that may affect the nervous system or circulation. In all experiments, subjects were instructed to abstain from caffeine, nicotine and alcohol for 12 hrs and 24 hrs, respectively, prior to the recording session. All participants received oral and written information about the procedures and risks involved, prior to the experiment. All participants gave written and informed consent in concordance with the Declaration of Helsinki.

3.2 Microneurography

All participants underwent recordings of peripheral sympathetic nerve activity. The procedure was performed with subjects lying semi-recumbent in a comfortable chair with the investigator probing the left peroneal nerve with an electrode. For further technical specifications of the recording equipment see **Paper 1**.

Nerve recordings were visually inspected for quality. This process focuses on assessing the signal to noise ratio of MSNA bursts, removing trials associated with artefacts (e.g. movement, muscle tension, electronic interference) and to look for signs that SSNA is present as well. In contrast to MSNA, SSNA is known to increase in relation to arousal, and may therefore severely contaminate measures of MSNA inhibition (Delius et al., 1972b; Wallin and Elam, 1997). Sympathetic fibers to skin and muscle are usually separated into different fascicles but may be found in proximity to each other. SSNA may be identified by being coupled to galvanic skin response (GSR, i.e. sweating) responses and have a longer duration than MSNA bursts.

During these sessions additional data was collected, namely electrocardiogram (ECG), BP, GSR, respiratory movement. The ECG consisted of three leads in a triangular pattern with Ag/AgCl electrodes. GSR was measured on the left palm at the thenar and hypothenar by two Ag/AgCl electrodes. Dynamic BP was measured continuously by a non-invasive method (Finometer model 1, cuff size medium; Finapres Medical System, Arnhem, The Netherlands) using

an inflatable volume-clamp around the left middle finger: mean arterial pressure (MAP) is estimated by an automated algorithm based on the arterial pulsations while taking into account the subject's age, gender, height and weight. Resting systolic and diastolic blood pressure (SBP, DBP) was measured in the supine position with an automated sphygmomanometer (Omega 1400, cuff size Adult 11; Invivo Research Inc, FL) on the left upper arm. The average of three consecutive measurements was taken as the final value and was used solely to determine that the participants were normotensive. Data from the same trials that were retained in MSNA were averaged and the mean arterial pressure for separate cardiac intervals was computed. The Finometer MAP readings of 'inhibitors' were compared to that of 'non-inhibitors' (defined below).

3.3 Stimulation

In all data collection procedures, except structural MRI, a stimulus was applied in order to induce responses in the nervous system. The stimulus consisted of a 0.2 - 0.8 ms electrical square wave pulse to the left index finger, and the strength was tuned according to a scale from 0 - 10 where 0 indicated no pain and 10 indicated intolerable pain. Participants were instructed to aim for a stimulus strength corresponding to a 7 on this pain scale. The reason for this subjective threshold is to produce a similar level of discomfort and thereby normalize the defensive arousal reaction between subjects.

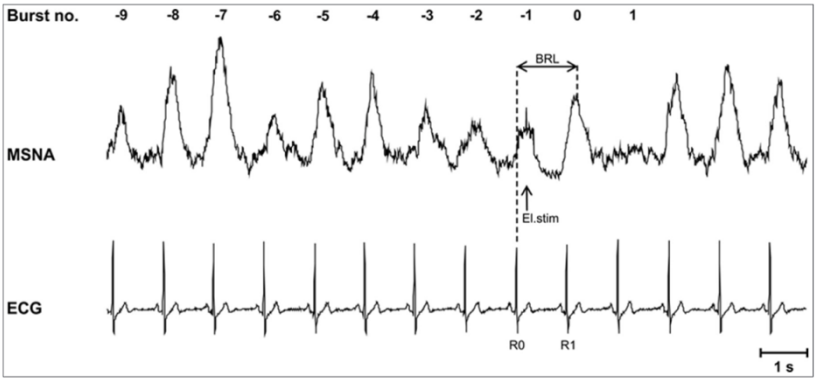

Figure 6. Rectified neurogram from a recording of MSNA illustrating the relationship in time between the baseline period -2 to -9 to electric stimulation at cardiac interval zero. The corresponding burst number has been adjusted according to the baroreflex latency (BRL). (Reprinted from: Lundblad LC. et al (2017). Sympathetic Nerve Activity in Monozygotic Twins: Identical at Rest but Not During Arousal. Hypertension, 69:964–969. https://doi.org/10.1161/HYPERTENSIONAHA.117.09079)

The electrical stimulus was locked to 200 ms after the R-wave because it has previously been shown to elicit the maximal amount of MSNA inhibition (Donadio et al., 2002a). Baseline was calculated as the average burst amplitude from burst -2 to -9 from all the included trials in an experiment, see figure 6. Post stimulus inhibition was then expressed as the average amplitude decrease in percent compared to baseline. Subjects that display 30 % or more reduction in mean post stimulus burst amplitude are defined as Inhibitors (cf Paper 1, and results 4.1).

The paradigms varied in the number of stimuli per trial. In **Paper 1** the number of trials was 60, with 30 trials containing a stimulation event and 30 did not contain a stimulus and were used as control trials. The order of trials was pseudo-randomized. For the stimulus trials, a single stimulus was used which is sufficient in order to induce inhibition of MSNA. In **Paper 2** the inhibition protocol was modified to be consistent with a previous publication (Donadio et al., 2002b) showing a concurrent effect on MAP, by using a train of five pulses locked to the heartbeat in the same way. However, the analysis of cortical responses needed a sufficient time window to examine induced responses, known to last for more than 1s. Therefore, in recordings with EEG and MEG in **Paper 2** and **Paper 3** the paradigm was based on the five stim paradigm but modified to three stimuli per trial repeated for 72 trials, with a space of one heartbeat in between, see figure 7. These multiple pulses then also allowed for the examination of adaptation between pulses.

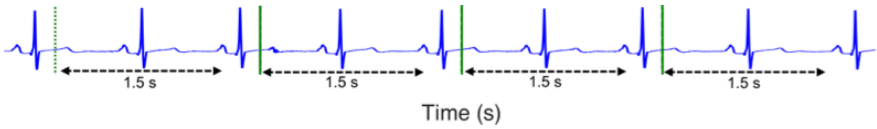

Figure 7. A schematic illustration of the 3-stim paradigm used in functional neuroimaging with MEG and EEG: three electric pulses, every other heartbeat, and a preceding baseline without stimulation.

3.4 MRI

Anatomical T1-weighted images of the brain were acquired through MRI for the cohort in **Paper 2**. Scans were performed in a Philips Gyroscan 3T Achieva and a 32 channel SENSE head coil with the following parameters: 180 sagittal slices, 1 mm^3 voxel size, flip angle 8°, TE 3.8 ms, TR 8.2 ms.

The MRI volumes were analysed with FreeSurfer (Dale et al., 1999; Fischl et al., 1999) using a region of interest (ROI) based approach. As described above,

the anterior cingulate cortex (ACC) and insula are important for evaluation and autonomic modulation and was therefore our main ROIs (Craig, 2002; Critchley et al., 2011; Dampney, 2018; Oppenheimer et al., 1992; Roy et al., 2012). Vogt and colleagues have described a four-region model of the cingulate cortex (Figure 8) based on receptor subtypes and structural and functional connections between regions. It is one of the most comprehensive assessments of cingulate architecture to date and describes an anterior, mid, posterior and retrosplenial portion (Palomero-Gallagher et al., 2009). The anterior cingulate corresponds to the rostral half of Brodmann Area (BA) 24, 32 and 25 and is subdivided into a pregenual region (BA 24, 32) and a subgenual region (BA 25) named for their relation to the genu of the corpus callosum. This description of an anterior cingulate corresponds to the rostral anterior cingulate label found in the Desikan-Killiany atlas in FreeSurfer (Desikan et al., 2006).

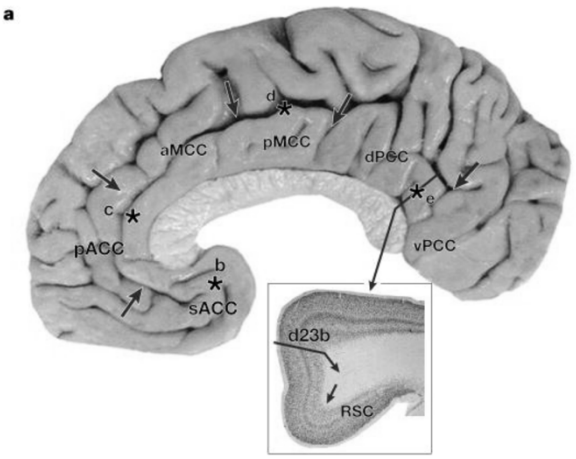

Figure 8. A four-region model of the cingulate gyrus based on immuno-histochemical investigations. ACC: anterior cingulate cortex (CC); MCC: mid; PCC: posterior; RSC: retrosplenial. (Adapted by permission from: Vogt BA. Pain and emotion interactions in subregions of the cingulate gyrus. Nat Rev Neurosci. 2005 Jul;6(7):533-44. doi: 10.1038/nrn1704)

The segmented images were co-registered to the "fsaverage" template and white matter boundaries and pial surfaces were reconstructed using the fully automated "recon -all" command. Surfaces were then parcellated into regions defined by the Desikan-Killiany atlas and mean cortical thickness was extracted for pre-selected ROIs, namely insula and rostral anterior cingulate cortex after applying a 10 mm FWHM Gaussian smoothing kernel. Cortical thickness was analyzed in relation to stimulus-induced inhibition of MSNA.

3.5 MEG

Data was recorded in an Elekta Neuromag® TRIUX system. Co-registration to individual MRIs was accomplished with a Polhemus FASTRACK system which allows for individually tailored source localization. Preprocessing was done in MNE python and included Independent Component Analysis (ICA) for removal of eye-blinks and cardiac artefacts (Gramfort et al., 2013; Gramfort et al., 2014) and analysis was done with the FieldTrip toolbox (Oostenveld et al., 2011). Source localization was done using the linearly constrained minimum variance beamformer method. Leadfields were constructed from volumetric ROIs from individual MRIs and the forward solution took into account the signal from all the conditions combined.

The insula and rostral anterior cingulate were chosen as ROIs for being part of the central autonomic network (Benarroch, 2012). Further analysis was done on the contralateral sensorimotor cortex where stimulus processing is known to occur. For each ROI only the vertices that displayed more than 60 % of peak power within the ROI was further analyzed, thus obtaining spatial specificity for the signal to be analyzed. The power spectral density of the post stimulus response was normalized to a baseline (a “pulse zero” equivalent to the stimulations but time-locked to two heart beats before pulse 1). The response in the frequency domain is expressed in dB i.e. a log scale and can be denoted event related synchronization or de-synchronization.

Results from a non-parametric cluster-based permutation test were interpreted and resulted in a window of interest in both time and frequency. Average change in power spectral density was computed using this exact window or as a time-series of the same frequency range (13 - 25 Hz) and was subsequently compared to MSNA-inhibition.

3.5.1 Oscillations

Analysis of MEG data is in principle performed in either the time domain which characterizes a response that is time-locked and phase-locked to an experimental event such as the electrical stimulations used to produce the results of this thesis, or in the frequency domain for a response that is time-locked but *not* phase-locked to the event. Time-domain analyses are done by averaging, through which a mean signal emerges while the non-phase locked signals are cancelled out. However, to characterize the non-phase-locked activity in neural oscillations, power as a function of frequency and time is calculated on a trial-by-trial basis, after which the oscillatory power of different frequencies may then be averaged only as a second step.

3.6 EEG

In **Paper 3** all participants underwent recordings with EEG. The main cohort was recruited with the purpose of validating and extending findings in **Paper 2** with a slightly more refined methodology through the use of simultaneous MNG and EEG. A standard EEG montage with 19 channels with electrode placement according to the international 10-20 system (Jasper, 1958) was chosen because of its common employ in clinical practice. This cohort was supplemented with the one from **Paper 2** in spite of some minor methodological differences. This was done in order to provide sufficient statistical power for evaluating a prediction model. In contrast to MEG, EEG is more susceptible to noise from muscle tension. Therefore, the analysis was based on a central electrode (Cz, cf figure 9) far from muscle tissue and the frequency analysis was focused on the lower beta band. In the auxiliary cohort there was an addition of an electrooculogram which somewhat facilitated the identification of artefacts identified by the independent component analysis. However, there was little doubt as to which components to reject in either cohort. Furthermore, due to its central location, ocular artefacts had a limited impact on the signal in the chosen Cz channel. All EEGs were referenced to a common average. Subsequently, data was cleaned through visual rejection of epochs containing artefacts of technical origin or from subject movement including transient muscle activity. Because transient episodes of arousal during sleep may cause increases in MSNA, (Hornyak et al., 1991) and because sleep affects attention, all recordings were screened for indication of decreased wakefulness. If the data rejection process resulted in an insufficient number of trials (< 30 in the EEG) the subject was excluded altogether.

During the preprocessing of the main cohort in **Paper 3** we had the option of matching the retained trials from microneurography and EEG recordings to ensure completely simultaneous data in the main cohort. However, demanding that a trial be clean in both EEG and MSNA recordings also resulted in a low number of remaining trials in several cases resulting in unacceptable loss of data (because two MSNA recordings were interrupted about halfway, up to about 50% of the planned trials would have been lost after rejection of gross artefacts in both recordings). We chose to prioritize volume of data and better signal-to-noise ratio over complete synchrony of data. Preprocessing was done in MNE, including ICA, (Gramfort et al., 2013; Gramfort et al., 2014) and frequency decomposition was performed with the Fieldtrip Toolbox (Oostenveld et al., 2011).

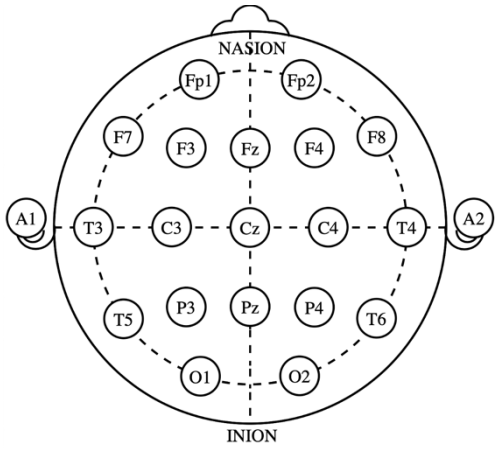

Figure 9. Placement and naming of electrodes according to the international 10-20 system defined by Jasper. (Wikimedia commons, public domain).

3.7 Statistics

In **Paper 1** the normal variability of 'post trigger' burst amplitude compared to the baseline of bursts was quantified from control conditions resulting in a threshold of ± 30 %. Pairs of monozygotic twins were compared to randomized pairs from the same cohort. A paired T-test was used to test for differences between rest and arousal within pairs. A 2-sample F-test for equal variances was used to test for differences between the twins and controls.

In **Paper 2** an outlier in MSNA inhibition was observed. This subject clearly displayed an excitatory burst behavior following some stimulations while the bursts were clearly judged to be MSNA in origin and not SSNA. No reason to exclude this subject was found. With this outlier included MSNA did not follow a normal distribution, and because parametric tests are sensitive to outliers we opted for a non-parametric correlation that makes no assumptions about the underlying distribution. The non-parametric cluster-based permutation test provides a flexible and unbiased way of testing for localized effects in several dimensions (Maris and Oostenveld, 2007). First an appropriate underlying test statistic is chosen (here Spearman's correlation) and the confluent clusters of significant tests are summarized and recorded. A Monte-Carlo simulation is then performed on the data to create a permutation distribution of clusters to which the clusters from the actual experiment are evaluated and determined to be significant or not. The test was employed on the diagrams of post stimulus change in power spectral density.

In order to increase the sensitivity of the study and limit the problem of multiple comparisons we opted for a ROI-based approach. Significant correlations were corrected with the modified Bonferroni-Holm procedure.

Blood pressure differences between inhibitors and non-inhibitors was computed using the Wilcoxon rank sum test on cardiac interval number 6 due to the expected maximum effect (Wallin and Nerhed, 1982).

In **Paper 3** the same non-parametric cluster-based test was used on power spectral density in time-frequency diagrams and on one dimensional time-series of average power in the beta band. Spearman's correlation coefficient was used for correlations between MSNA-inhibition and average power. Correction for multiple comparisons was done with the modified Bonferroni-Holm procedure. The binary classification performance was summarized, as is common, with a receiver-operating-characteristics curve of sensitivity and false positive rate by manual coding in MatLab (The Math Works Inc., Massachusetts). From a clinical standpoint we hypothesize that it would be of greater interest to accurately classify non-inhibitors and so this group defined the cases.

4 RESULTS

4.1 Paper 1

In **Paper 1**, eight pairs of monozygotic male twins were examined (Lundblad et al., 2017). Resting activity was quantified as BI and BF and intra-pair differences were calculated. The within-pair absolute difference in BI for the twins was 8.3 ± 1.03 as compared to 19.7 ± 5.8 bursts/100 heart beats for the randomized control pairs: the resting BI was found to be more similar within twins compared to controls ($p<0.001$). Similarly, the within-pair difference in BF was 4.5 ± 1.1 and 12.7 ± 2.9 bursts/min for the twins and controls respectively ($p=0.002$). The within-pair ratios of resting BI (figure 10) were also significantly different between twins and controls (0.87 ± 0.002 vs 0.73 ± 0.07, F-test, $p=0.002$). In contrast to resting activity, the within-pair ratios for the arousal induced inhibition (figure 10), 0.56 ± 0.11 versus 0.46 ± 0.11, were not statistically different between twins and controls respectively (F-test, $p=0.939$).

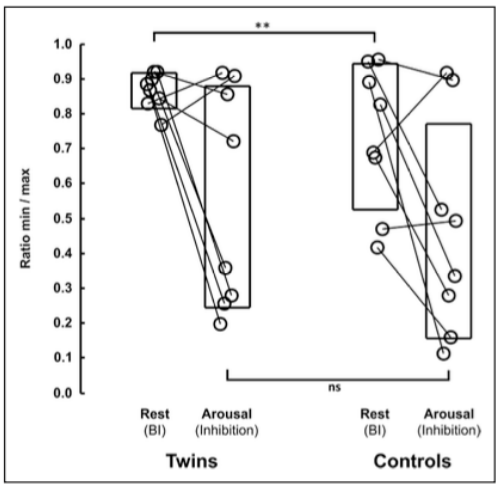

*Figure 10. Within pair ratios of MSNA during rest and arousal in both monozygotic twins and randomized control pairs. ** p < 0.01; ns: non-significant. (Reprinted from: Lundblad LC, et al. (2017). Sympathetic Nerve Activity in Monozygotic Twins: Identical at Rest but Not During Arousal. Hypertension, 69:964–969. https://doi.org/10.1161/HYPERTENSIONAHA.117.09079)*

On a further note, a level of normal variability in post stimulus burst amplitude, compared to baseline, was determined from control conditions. This normal variability showed that at least 30% reduction in burst amplitude post stimulus is necessary in order to determine a significant degree of MSNA inhibition. This limit was used to define Inhibitors and non-Inhibitors in **Paper 2** and **Paper 3**.

4.2 Paper 2

In **Paper 2** post stimulus blood pressure was found to be different between inhibitors (n=7) and non-inhibitors (n=8)(p=0.021, Paper 2 fig 1), which was in line with what has been reported previously (Donadio et al., 2002b). The MSNA inhibitory reaction was also found to be correlated to estimates of cortical thickness in the anterior cingulate cortex (n=20, p=0.004, Paper 2 fig 2). Functional changes in the oscillatory activity were assessed via MEG in pre-selected ROIs. An increased oscillatory activity was found in both the insula, the anterior cingulate and the sensorimotor cortex, emergent mainly within the beta band and was consistent with pre-existing descriptions of stimulus-induced beta rebound (Paper 2, fig 2, 3, 4). The level of beta rebound was found to be correlated to stimulus-induced MSNA inhibition in both the anterior cingulate ($p< 0.001$) and the sensorimotor cortex ($p< 0.001$) following stimulus no. 2 and 3 (Paper 2, fig 2 and 4), but not in the insular cortex.

In this study, an outlier was observed with MSNA inhibition equal to -132 %, i.e. an increase in mean burst amplitude. Normal variability is observed up to ± 30 %, but there was no compelling reason to exclude this observation and so it was retained. Checking the results after removing the outlier did not change the conclusions of the results from either the functional MEG or structural MRI analysis.

4.3 Paper 3

In **paper 3** the findings regarding beta rebound in MEG were assessed with EEG. The beta band was split into low beta 13-20 Hz and high beta 20-30 Hz, considering how EEG is more readily contaminated by myogenic noise. A correlation was found between stimulus-induced MSNA inhibition and beta rebound power in the low beta band following pulse 3 ($n=37$, $p=0.021$). This relationship was explored further by means of binary classification into inhibitor or non-inhibitor subgroups based on beta rebound power. The performance was assessed with a receiver-operating characteristic curve which showed a modest accuracy of 0.70 (AUC = 0.70, sensitivity = 0.74, false positive rate = 0.33) presented in paper 3, figure 2.

Some participants displayed short drops in wakefulness. Such episodes were removed and no systematic effect was discernable but can be explained by the low number of trials removed.

Investigation of individual responses in EEG highlight interindividual differences in stimulus induced synchronization. In figure 11, the bottom three rows are some of the most prime examples of what can be described as (most likely neurogenic) beta rebound in this sample. The subjects display variable peak frequencies from low to high portions of the beta band. One subject also shows a sporadic signal change in the higher frequencies, without the preceding desynchronization which may therefore indicate a more noise-like pattern. Concentrated responses may also be intermixed with streaks of transient high frequency change in power. This illustrates the difficulties of truthfully describing the beta band with EEG, and high frequencies in particular, as it is hard to discriminate between myogenic and neurogenic change in power. However, by cutting the high beta band one will also fail to capture the response in subjects with high peak frequencies.

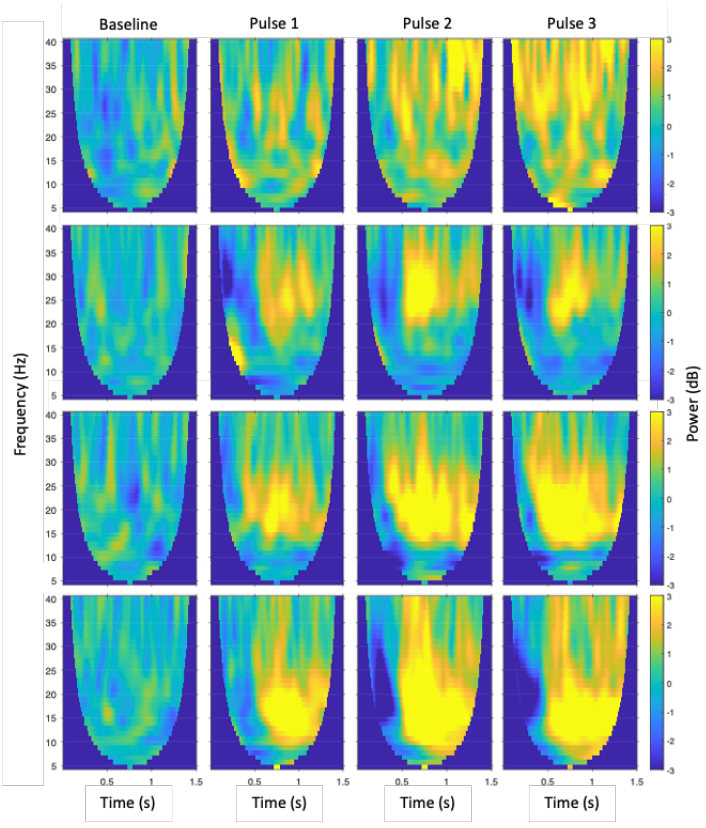

Figure 11. 1st row: subject is displaying lack of clear desynchronization and beta rebound, interpreted as a noise-like pattern. 2nd row: beta rebound with high peak frequency. 3rd row: beta rebound with mid peak frequency. 4th row: beta rebound with low peak frequency.

5 DISCUSSION

5.1 Summary

The results confirmed the genetic influence on resting MSNA and ascertained that the sympathetic response to arousal is not rigid but may, instead, to a large degree, be influenced by environmental factors. The prevalence of inhibition is around 50-75 % across these studies, as in previous work, and the tendency in the Inhibitor group for a buffering of the stimulus induced blood pressure increase was replicated. The sympathetic response was linked to induced oscillatory responses recorded with MEG in areas involved in sensory processing or higher cognitive function and autonomic control. Furthermore, inhibition correlated to cortical thickness in the ACC, an index of long-term plasticity in the cerebral cortex. Finally, we show that the functional response in the sensorimotor cortex was weakly discernable also with EEG, but the method performs poorly as a non-invasive alternative to microneurography.

5.2 CAN and environmental stress

In humans, sympathetic resting activity to muscle vasculature is highly determined by genotype, as shown previously and replicated in **Paper 1** (Wallin et al., 1993). Results also show that the arousal reaction (defense related inhibition) is not genetically determined but varies within monozygotic twin pairs. The good reproducibility in conjunction with the coupling of inhibition to longer stress speaks to an underlying personal trait (Donadio et al., 2002b; Donadio et al., 2012). Generally speaking, the neural and circulatory outcome associated with defense-reactions can be shaped by past life-experiences (Korner, 2007). While the background history of the current twin cohort was very homogenous (Lundblad et al., 2017), it is possible that more or less subtle differences in psychological history could explain the discordant pairs.

In **Paper 2** we investigated the most likely cortical regions to be involved in processing of environmental stimuli and that are known to affect circulatory homeostasis. Stimulation of the insula is known to elicit cardiac and vascular changes (Oppenheimer et al., 1991; Oppenheimer et al., 1992). The Insula is also viewed as a site for interoceptive awareness (Craig, 2002). However, neither functional or structural correlations to MSNA inhibition were found. Although evidence was seen that the signal was processed and relayed through here (Paper 2 fig 3), the null finding in the insula suggests that learning and/or response selection occurs elsewhere.

As hypothesized, in **Paper 2**, a link was found between processes in the anterior cingulate and inhibition of MSNA. Although the ACC has been linked to autonomic responses, the observed cortical response is not the cause of the MSNA inhibition to the initial arousal stimulus. MSNA inhibition is elicited in immediate proximity to the given stimulus either on the same heart beat or the next. The correlation to the cortical response however is delayed and appears in response to the second and third stimulus. Therefore, it suggests some other link between what appears to be low-level arousal and high-level cortical processes.

The ACC is one brain region known to be involved in threat assessment and complex evaluation and generation of affective meaning (Roy et al., 2012). We hypothesized that, as a result of past exposure, an implicit learning in the ACC would influence synaptic density and cortical thickness. This was supported by our data in **Paper 2** that showed that increased grey matter was correlated to a tendency for less MSNA inhibition. Possibly, the ACC has the potential to modify or exercise a tonic modulation of lower-level circuits. It has previously been shown that perceived social standing in immigrants covaries with cortical thickness in the ACC (Gianaros et al., 2007). The ACC is implicated not only in chronic, but also acute social stress (Wager et al., 2009). Furthermore, the ACC (infra- and prelimbic cortex in rodents) is implicated in shaping goal-oriented defensive behavior through connections and interactions with the amygdala (LeDoux and Daw, 2018). This suggests that MSNA-inhibition, as a first step in a defense cascade (Kozlowska et al., 2015), is related to defense in a broad sense. The epidemiological evidence for a neural and social component in cardiovascular risk is compelling (Hollenberg et al., 1997; Timio et al., 1997; Timio et al., 1999), and may be mediated through processes in the ACC brain region (Lederbogen et al., 2011) providing a clinical outlook for defense-related inhibition of MSNA.

The perspectives on effects from stress and emotion on activity in the ACC can be broadened further. For example, chronic stress in mice alters the intrinsic oscillatory power within the ACC, in several frequencies including the beta band (Ito et al., 2020) and synaptic plasticity in the ACC was enhanced in stressed mice which was likely due to reduced GABA (gamma-aminobutyric acid)-related inhibition (Ito et al., 2010). Furthermore, previous adverse life events affect metabolic activity in the ACC during a Stroop task (Godinez et al., 2016). This indicated a need for more effort in making sense of information in those who were exposed to environmental stress during their formative youth. The pathophysiology of depressive symptoms is related to chronic stress and aberrant 5-hydroxytryptamine signaling (Dean and Keshavan, 2017; Kendler et al., 1999), likely in the subgenual ACC (Palomero-Gallagher et al.,

2009) and the brainstem where serotonergic activity has been found to modulate cardiovascular responses to acute stressors (Horiuchi et al., 2011). Incidentally, beta oscillations in the subgenual ACC were found to be altered in humans with clinical depression (Merkl et al., 2016).

The fact that this particular arousal reaction in the sympathetic nervous system is shown not to be rigid means that it can be subject to change. The genetic contribution to hypertension has been estimated to 30 % and the environmental contribution to 55 % (Korner, 2007). A low genetic determination raises future interest and clinical potential of the arousal reaction pattern under study here since it opens the possibility for both studying dynamic processes over time as well as performing targeted interventions. However, it remains to be seen how slow or quick they are to change given the proper stimulus, or if there is a certain critical period in life during which conditioning is facilitated. As a final note however, one may observe a tendency for two separate clusters in fig 10, with some twins that differ and some that are more similar in their arousal response. A limited sample size notwithstanding, one may speculate on whether or not it signifies some level of heredity with incomplete penetrance in these concordant pairs.

5.3 Rolandic response

The response known as beta rebound is a well-known phenomenon as a result of somatosensory stimulation as well as movements (Cassim et al., 2001; Cheyne, 2013; Salenius et al., 1997). The functional significance of this rhythm is still under debate, and some have suggested that oscillations reflect interregional communication, however beta is also thought likely to mean an active inhibitory state, a maintaining of the status quo (Engel and Fries, 2010; Kilavik et al., 2013). This inhibition of the cortex is supported by its relation to the inhibitory neurotransmitter GABA which is released from interneurons in the cortex (Gaetz et al., 2011; Muthukumaraswamy et al., 2013).

The oscillations in response to pulse 2 and 3 are correlated to inhibition of MSNA from the first stimulus. The beta rebound in the sensorimotor cortex and the similar response in the ACC could be indicative of a coordinated response pattern involving several systems. The evaluative role of the ACC might be linked to a ‘decision’ on sensory filtering of further incoming stimuli. Inhibition of MSNA then reveals a differential autonomic response related to such evaluation. Such theories on a concerted response need to be supported by more experiments.

5.4 Non-invasive prediction with EEG

Paper 3 attempted to exploit the correlates in the sensorimotor region with EEG. Tendencies for correlations between MSNA inhibition and beta oscillatory power, similar to that observed with MEG were seen. Inhibitors tended to have a stronger beta rebound response. The correlations were weak however, and only detected in relation to pulse 3, whereas in MEG there were significant correlations in both pulse 2 and 3. Furthermore these correlations were only apparent in the lower beta band 13-20 Hz. It is a well-known problem that EEG recordings are contaminated by muscle noise, and that this noise is predominant in frequencies above 20 Hz (Goncharova et al., 2003; Keren et al., 2010; Whitham et al., 2007). In particular the temporal muscle is a large muscle located at the temples and is often a source of concern (Yilmaz et al., 2014). This is a plausible explanation for this discrepancy between high and low beta. The choice of threshold is an arbitrary one as in reality the strength of muscle noise increases gradually with frequency. Furthermore, the MEG results were interpreted to emphasize frequencies up to 25 Hz, so the truncated range is also likely to blame, in part, for the weaker correlations.

Several other important differences also exist between the modalities. The EEG analysis was carried out at the sensor level. That is a particular channel was selected, namely Cz found at the vertex of the head. The choice was based on a desire to capture the response in the central sulcus but also avoid muscle artefacts as much as possible. EEG differs greatly from the source level analysis in MEG in which individual MRIs are used to pinpoint activity. Source level analysis can be performed with EEG as well but because it measures extracellular volume currents the method is inherently limited in spatial sensitivity (Ding and Yuan, 2013; Puce and Hämäläinen, 2017). We also opted for a standard clinical 19 channel montage as a feasibility study for future applications.

Furthermore, the difference in sensitivity for different parts of the cortex might have played a role (cf Intro 1.4). And as mentioned above, MEG measures the magnetic fields caused by synaptic currents and EEG measures the extracellular volume currents set in motion by the neural activity. The MEG sensors are active sensors operating independently of one another while EEG electrodes require a reference (Lopes da Silva, 2010; Parkkonen, 2010). A common average reference was used in this analysis. There is the option of choosing a bipolar lead, but it is unclear which other electrode should be the reference electrode. Another option is the Laplacian (nearest neighbor) montage which tries to isolate activity in a choice electrode from the surrounding neighbors. With respect to attempts of handling myogenic noise

the success of this approach has varied (Fitzgibbon et al., 2013; Goncharova et al., 2003).

Myogenic noise is of great concern to many EEG researchers and many papers have been published with various algorithms and procedures to handle this problem. However, it is difficult to discern any real consensus on the topic (Liu et al., 2019; McMenamin et al., 2011; Olbrich et al., 2011; Shackman et al., 2009).

Unfortunately, the simultaneous recordings of both MSNA and EEG, were tiresome for some participants. Fearing that instances of arousal during sleep stage 2 would lead to transient sympathetic excitation (Hornyak et al., 1991), each recording was screened for signs of sleep and each identified trial was rejected together with the preceding and following trial. However, we quantified the change in MSNA before and after removal of sleep and concluded that the differences were negligible. Therefore, we are confident that the data analyzed is of good quality.

For the binary classification problem to be addressed we had to have a substantial number of observations. The two cohorts were deemed similar enough that this would not pose a problem. The results presented are for non-inhibitors defined as cases, but switching to inhibitors does not make a big difference - the performance curve (Paper 3 fig 2) would retain its shape but be flipped along the diagonal. The accuracy describes the combined sensitivity and false positive rate of a particular threshold. A value of 0.70 as reported means 70% were correctly classified which can be considered mediocre - a classifier of no skill, equivalent to a coin toss, would still result in 50% correct classification.

The choice to limit the beta spectrum to 20 Hz and below means that any true neurogenic response in the high beta band above 20 Hz will be missed. Inspection of individual time-frequency power spectrograms (Results, fig 11) revealed a considerable interindividual variability in peak frequency. Assuming some of these peaks were of neurogenic in origin this desire for increased specificity also leads to a decrease in sensitivity. This is an important aspect to consider also for future studies with MEG.

5.5 Limitations

The studies in this thesis were all done on male participants. It is of course important to investigate whether these findings hold true in the female population as well, concerning defense reactions and the theories of how the cardiovascular system responds to environmental stimuli. However, from a clinical standpoint it is also important to note that men and women have different natural histories when it comes to sympathetic activity during a lifetime as well as hypertension risk (Charkoudian, 2001; Joyner et al., 2016), and so the desire to develop and validate a biomarker must take these differences in the two populations into consideration. Furthermore, the cross-sectional nature of the studies means that the interpretation of cortical thickness as a result of plasticity is limited. Another limitation is the focus on specific brain regions as in order to more fully understand the physiology behind MSNA inhibition and defense reactions it might be enlightening to examine more areas of the brain. Outliers often raise concerns about the statistical robustness of a correlation. The use of non-parametric statistics should alleviate such concerns and the results in **Paper 2** were significant even with the outlier observation removed from the data.

5.6 Outlook

An unstable environment marked by repeated exposure to stressful stimuli can lead to persistent increases in SNA and BP (Henry et al., 1993) even after the stimulus has receded. This and other findings are also consistent with the idea of neural and behavioral mechanisms (Lawler et al., 1984; Li et al., 1997). The study by Timio also strongly suggests a neural genesis to hypertension in humans (Timio et al., 1988; Timio et al., 1999; Timio et al., 1999) and perhaps it is not the strength of the stimulus but rather its recurring nature that may be most important (Folkow, 1991), as is common in a modern urban environment.

In human hypertension, several studies show elevated levels of MSNA (Grassi et al., 2018; Yamada et al., 1989), but the great interindividual variability in resting levels of MSNA makes predicting hypertension risk from MSNA non-feasible. However, it is possible that dynamic measures of SNA may prove useful as a predictor for future hypertension, or may shine more light on the development of hypertension and cardiovascular risk (Chida and Steptoe, 2010). Perhaps the general responsiveness to arousal in the nervous system has something to tell us on this topic.

6 CONCLUSIONS

From the study on monozygotic twins, we conclude that the arousal response is not determined by a particular genotype and therefore it will be interesting to examine the factors that may push a person's sympathetic and blood pressure reactivity across the spectrum. Such a measure should be considered interesting in relation to cardiovascular health for which sympathetic resting activity has not provided sufficient explanations. This body of work has provided some clues as to the centrally coupled mechanisms of MSNA inhibition. The involvement of the ACC strengthens the belief that this is a response related to defense reactions in general and the strong correlation to the Rolandic cortex provides new perspectives on the interplay between autonomic and sensorimotor processing. However, more work is needed in order to understand the processes and structures involved, elucidating their purpose in defense reactions. While a standard clinical EEG was not a convincing approach, other avenues using MEG are still open for a future non-invasive characterization of defense related inhibition. Figure 12 provides a graphical overview of the ideas and results contained in this thesis.

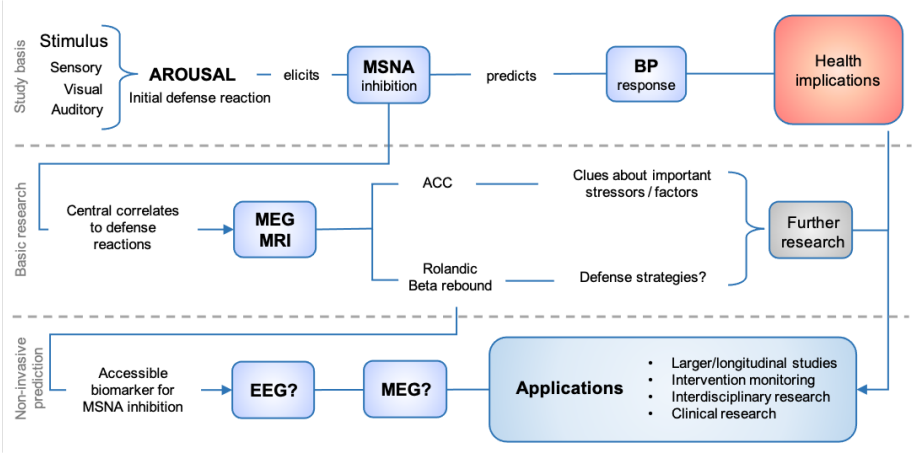

Figure 12. Flowchart illustrating how cortical indices of defense-related sympathetic inhibition were measured with neuroimaging with the aim of facilitating future studies on the topic as well as approaching the possible health implications of the response.

7 FUTURE PERSPECTIVES

The results from the brain imaging analyses have provided interesting clues to the interplay between high-level cortical processes and basic cardiovascular control. However, the use of preselected regions limits the mechanistic understanding of the response. It would be interesting to conduct studies with the aim of elucidating the entire flow of information but requires more refined methods. A connectivity analysis of the whole brain would be enlightening, but challenging due to the multidimensional data involved. Such a study would benefit from incorporating other sensory modalities as well to answer whether the responses seen in ACC or the proposed filtering of sensory information and/or maintaining of motor programs in the Rolandic cortex are independent of stimulus modality and thus indicative of a generalized defense reaction.

The lackluster ability of a simple EEG to correctly classify subjects' MSNA inhibition is disappointing. But the strong correlations with MEG data remain and can still potentially be exploited as a means of non-invasive prediction. More work is needed to validate a classifier though. However, the practical gains should be greater if these results could also be replicated using next generation MEG systems operating at higher temperatures (High-Tc SQUID (Boto et al., 2017; Pfeiffer et al., 2020)). This is prognosticated to decrease overhead costs of running a lab, and provide increased signal to noise ratio due to closer positioning to the scalp. Increased SNR should result in increased accuracy and possibly new correlates, or allow for shorter protocol time from a decreased number of trials with preserved accuracy. Other effector organs controlled by the sympathetic nervous system include the heart which could also possibly contribute to a more complex prediction model.

The evidence for structural adaptations in the ACC measured in cortical thickness would be strengthened by a longitudinal design for characterizing MSNA inhibition and cortical thickness in the ACC, with follow-up measurements after some six months for example. To enforce the environmental stimulus perhaps a group of medical students, with a rural background and fresh out of high-school, could be examined at enrollment and re-examined at the end of their first semester to see how they have adapted to their new life. The findings in the ACC should also be of interest to psychologists. Studies that correlate defense reactions in the sympathetic nervous system to measures from neuroimaging from a behavioral point of view would be most interesting. Experimental interventions could entail mental and social stress. Psychoaffective indices could be correlated to degree of inhibition. In general, the combination of microneurography and

neuroimaging modalities is likely to shed more light on the causes and modulators of this inhibition phenomenon.

There is also an urgent need for studies on females. A study on young females is currently underway. This should be complemented with post-menopausal females whose sympathetic and cardiovascular risk profile is more akin to the male population (Joyner et al., 2016; Reckelhoff, 2001).

ACKNOWLEDGEMENTS

This work was made possible by the support of the Knut and Alice Wallenberg foundation, Swedish Research Council, Swedish Childhood Cancer Foundation, Sahlgrenska Academy.

I've always wanted to try my hand at research, but wasn't quite sure what I was getting into when I started this journey. Although it has been challenging and lots of hard work, it has also been most rewarding. Learning all these wonderful methods and thinking about how to combine them has been very engaging and I consider myself privileged for having been given this opportunity. I am especially grateful for working with such enthusiastic and esteemed colleagues in the field – your qualities are what enabled me to grow.

So, a huge thank you to Mikael Elam for taking me on and guiding me through these years, always with excellent advice and generous support and knowledge that can only come from a place of great experience, empathy and mental acuity. Thanks for your energy and enthusiasm and desire to make a difference.

A big thanks to my co-supervisors for your generous support in all aspects of this work. Thanks to Linda Lundblad for your skill and patience in helping me learn microneurography and brain morphometry, and for all the funny chronicles of a dog owner's life. Thanks to Justin Schneiderman for helping me with the more complicated aspects of functional imaging, and your positive outlook and drive is a real inspiration.

Thank you to Tomas Karlsson for being a rock-solid source of information and advice on all things analytical and being a good office mate and friend, helping me out whenever needed. And thank you to Gunnar Wallin, a good friend who offers insight and advice and whom it has been a privilege to get to know. Sharing your interests in local history was a nice change of pace. And thanks to Bushra for your friendship and assistance in teaching me how to code, I promise to have lots of goodies in store for when you drop by.

Thanks to the other co-authors Göran Starck, Daniel Lundqvist, Robert Oostenveld for your essential contributions to the work.

Thank you to all the participants for making these studies possible, and with whom I have had many long and interesting conversations during preparation times.

Thank you to Göran Pegenius, whose oak saplings in the window I have admired from a distance, for being nice enough to show me how to use the TMS system, a neat little

bonus to a PhD packed with methodological knowledge already. And thank you to Samuel Klemetz and Joakim Strandberg for the entertaining practice sessions.

Thanks to summer research students Jonatan Bengtsson and Lukas Hilgendorf, I have learned from your studies as well.

Thanks to the administrative staff Maria Björkevik, Kirsten Toftered, Hanna Karlsson and others who have been instrumental, especially in the last months before this work was printed.

I also want to thank Rolf Heckemann and Holger Nilsson for their valuable thoughts on the work.

Thanks to Johan Kling and Stefan Nivall who have provided under the hood assistance regarding data acquisition, questions from the group and various other hang-ups. And thanks to the rest of the staff at KNF for any other interactions we have had. Thanks to the others at MedTechWest and Medicinareberget who have also contributed.

Thank you to all my friends for providing welcome distractions and support during this time. A special thanks to my PhD-student friends Jonathan, Johan and Bushra. And to my wonderful sister Henrietta and to Emil for being great friends, and for brightening the last few months with updates on Juno's latest achievements.

And finally, to my dear parents, to whom I truly want to say 'thank you'. This work is dedicated to you.

- Tack, för allt ni har gjort för mig

REFERENCES

Abela E, Seiler A, Missimer JH, Federspiel A, Hess CW, Sturzenegger M, Weder BJ, Wiest R. (2015). Grey matter volumetric changes related to recovery from hand paresis after cortical sensorimotor stroke. *Brain Struct Funct*, 220:2533–2550.

Amunts K, Schlaug G, Jancke L, Steinmetz H, Schleicher A, Dabringhaus A, Zilles K. (1997). Motor cortex and hand motor skills: structural compliance in the human brain. *Hum Brain Mapp*, 5:206–15.

Ashburner J, Friston KJ. (2000). Voxel-based morphometry--the methods. *NeuroImage*, 11:805–821.

Baron JC, Chételat G, Desgranges B, Perchey G, Landeau B, de la Sayette V, Eustache F. (2001). In vivo mapping of gray matter loss with voxel-based morphometry in mild Alzheimer's disease. *NeuroImage*, 14:298–309.

Benarroch EE. (2012). Central Autonomic Control. In: Robertson, D, Biaggioni, I, Burnstock, G, Low, PA, Paton, JFR, editors.. *Primer on the Autonomic Nervous System (Third Edition)*, . San Diego: Academic Press. pp 9–12. https://www.sciencedirect.com/science/article/pii/B9780123865250000020.

Boto E, Meyer SS, Shah V, Alem O, Knappe S, Kruger P, Fromhold TM, Lim M, Glover PM, Morris PG, Bowtell R, Barnes GR, Brookes MJ. (2017). A new generation of magnetoencephalography: Room temperature measurements using optically-pumped magnetometers. *NeuroImage*, 149:404–414.

Cardinale F, Chinnici G, Bramerio M, Mai R, Sartori I, Cossu M, Lo Russo G, Castana L, Colombo N, Caborni C, De Momi E, Ferrigno G. (2014). Validation of FreeSurfer-estimated brain cortical thickness: comparison with histologic measurements. *Neuroinformatics*, 12:535–42.

Carter JR, Kupiers NT, Ray CA. (2005). Neurovascular responses to mental stress. *J Physiol*, 564:321–327.

Carter JR, Ray CA. (2009). Sympathetic neural responses to mental stress: responders, nonresponders and sex differences. *Am J Physiol Heart Circ Physiol*, 296:H847-853.

Cassim F, Monaca C, Szurhaj W, Bourriez J-L, Defebvre L, Derambure P, Guieu J-D. (2001). Does post-movement beta synchronization reflect an idling motor cortex?. *Neuroreport*, 12:3859–3863.

Charkoudian N. (2001). Influences of female reproductive hormones on sympathetic control of the circulation in humans. *Clin Auton Res*, 11:295–301.

Cheyne DO. (2013). MEG studies of sensorimotor rhythms: a review. *Exp Neurol*, 245:27–39.

Chida Y, Steptoe A. (2010). Greater cardiovascular responses to laboratory mental stress are associated with poor subsequent cardiovascular risk status: a meta-analysis of prospective evidence. *Hypertens Dallas Tex 1979*, 55:1026–1032.

Craig AD. (2002). How do you feel? Interoception: the sense of the physiological condition of the body. *Nat Rev Neurosci*, 3:655–666.

Critchley HD, Nagai Y, Gray MA, Mathias CJ. (2011). Dissecting axes of autonomic control in humans: Insights from neuroimaging. *Auton Neurosci Basic Clin*, 161:34–42.

Cui J, Blaha C, Herr MD, Drew RC, Muller MD, Sinoway LI. (2015). Limb suction evoked during arterial occlusion causes systemic sympathetic activity in humans. *Am J Physiol Regul Integr Comp Physiol*, 309:R482-488.

Dahlstroem A, Fuxe K. (1964). Evidence for the existence of monoamine-containing neurons in the central nervous system. I. Demonstration of monoamines in the cell bodies of brain stem neurons. *Acta Physiol Scand Suppl*, :SUPPL 232:1-55.

Dale AM, Fischl B, Sereno MI. (1999). Cortical surface-based analysis. I. Segmentation and surface reconstruction. *Neuroimage*, 9:179–94.

Dampney RA. (1994). Functional organization of central pathways regulating the cardiovascular system. *Physiol Rev*, 74:323–364.

Dampney RA. (2018). Emotion and the Cardiovascular System: Postulated Role of Inputs From the Medial Prefrontal Cortex to the Dorsolateral Periaqueductal Gray. *Front Neurosci*, 12:343.

Dampney RA, Furlong TM, Horiuchi J, Iigaya K. (2013). Role of dorsolateral periaqueductal grey in the coordinated regulation of cardiovascular and respiratory function. *Auton Neurosci Basic Clin*, 175:17–25.

Dampney RA, Michelini LC, Li D-P, Pan H-L. (2018). Regulation of sympathetic vasomotor activity by the hypothalamic paraventricular nucleus in normotensive and hypertensive states. *Am J Physiol Heart Circ Physiol*, 315:H1200–H1214.

Dean J, Keshavan M. (2017). The neurobiology of depression: An integrated view. *Asian J Psychiatry*, 27:101–111.

Delius W, Hagbarth KE, Hongell A, Wallin BG. (1972a). General characteristics of sympathetic activity in human muscle nerves. *Acta Physiol Scand*, 84:65–81.

Delius W, Hagbarth KE, Hongell A, Wallin BG. (1972b). Manoeuvres affecting sympathetic outflow in human skin nerves. *Acta Physiol Scand*, 84:177–186.

Desikan RS, Ségonne F, Fischl B, Quinn BT, Dickerson BC, Blacker D, Buckner RL, Dale AM, Maguire RP, Hyman BT, Albert MS, Killiany RJ. (2006). An automated labeling system for subdividing the human cerebral cortex on MRI scans into gyral based regions of interest. *NeuroImage*, 31:968–980.

DiMicco JA, Stotz-Potter EH, Monroe AJ, Morin SM. (1996). Role of the dorsomedial hypothalamus in the cardiovascular response to stress. *Clin Exp Pharmacol Physiol*, 23:171–176.

Ding L, Yuan H. (2013). Simultaneous EEG and MEG source reconstruction in sparse electromagnetic source imaging. *Hum Brain Mapp*, 34:775–795.

Donadio V, Kallio M, Karlsson T, Nordin M, Wallin BG. (2002a). Inhibition of human muscle sympathetic activity by sensory stimulation. *J Physiol*, 544:285–92.

Donadio V, Karlsson T, Elam M, Wallin BG. (2002b). Interindividual differences in sympathetic and effector responses to arousal in humans. *J Physiol*, 544:293–302.

Donadio V, Liguori R, Elam M, Karlsson T, Giannoccaro MP, Pegenius G, Giambattistelli F, Wallin BG. (2012). Muscle sympathetic response to arousal predicts neurovascular reactivity during mental stress. *J Physiol*, 590:2885–2896.

Donadio V, Liguori R, Elam M, Karlsson T, Montagna P, Cortelli P, Baruzzi A, Wallin BG. (2007). Arousal elicits exaggerated inhibition of sympathetic nerve activity in phobic syncope patients. *Brain*, 130:1653–62.

El Sayed K, Macefield VG, Hissen SL, Joyner MJ, Taylor CE. (2018). Blood pressure reactivity at onset of mental stress determines sympathetic vascular response in young adults. *Physiol Rep*, 6:e13944.

Elam M, Macefield V. (2001). Multiple firing of single muscle vasoconstrictor neurons during cardiac dysrhythmias in human heart failure. *J Appl Physiol Bethesda Md 1985*, 91:717–724.

Engel AK, Fries P. (2010). Beta-band oscillations—signalling the status quo?. *Curr Opin Neurobiol*, 20. Cognitive neuroscience:156–165.

Esler M. (2011). The sympathetic nervous system through the ages: from Thomas Willis to resistant hypertension. *Exp Physiol*, 96:611–622.

Esler M, Jennings G, Korner P, Willett I, Dudley F, Hasking G, Anderson W, Lambert G. (1988). Assessment of human sympathetic nervous system activity from measurements of norepinephrine turnover.. *Hypertension*, 11:3–20.

Fagius J. (2003). Sympathetic nerve activity in metabolic control--some basic concepts. *Acta Physiol Scand*, 177:337–343.

Fagius J, Wallin BG. (1980). Sympathetic reflex latencies and conduction velocities in normal man. *J Neurol Sci*, 47:433–448.

Fagius J, Wallin BG, Sundlöf G, Nerhed C, Englesson S. (1985). Sympathetic outflow in man after anaesthesia of the glossopharyngeal and vagus nerves. *Brain J Neurol*, 108 (Pt 2):423–438.

Fischl B, Sereno MI, Dale AM. (1999). Cortical surface-based analysis. II: Inflation, flattening, and a surface-based coordinate system. *Neuroimage*, 9:195–207.

Fitzgibbon SP, Lewis TW, Powers DMW, Whitham EW, Willoughby JO, Pope KJ. (2013). Surface Laplacian of central scalp electrical signals is insensitive to muscle contamination. *IEEE Trans Biomed Eng*, 60:4–9.

Folkow B. (1991). Mental “stress” and hypertension. Evidence from animal and experimental studies. *Integr Physiol Behav Sci Off J Pavlov Soc*, 26:305–308.

Fonkoue IT, Carter JR. (2015). Sympathetic neural reactivity to mental stress in humans: test-retest reproducibility. *Am J Physiol Regul Integr Comp Physiol*, 309:R1380-1386.

Fontes M a. P, Xavier CH, de Menezes RCA, Dimicco JA. (2011). The dorsomedial hypothalamus and the central pathways involved in the

cardiovascular response to emotional stress. *Neuroscience*, 184:64–74.

Gaetz W, Edgar JC, Wang DJ, Roberts TPL. (2011). Relating MEG measured motor cortical oscillations to resting γ-aminobutyric acid (GABA) concentration. *NeuroImage*, 55:616–621.

Gianaros PJ, Horenstein JA, Cohen S, Matthews KA, Brown SM, Flory JD, Critchley HD, Manuck SB, Hariri AR. (2007). Perigenual anterior cingulate morphology covaries with perceived social standing. *Soc Cogn Affect Neurosci*, 2:161–73.

Gloor P. (1969). Hans Berger on Electroencephalography. *Am J EEG Technol*, 9:1–8.

Godinez DA, McRae K, Andrews-Hanna JR, Smolker H, Banich MT. (2016). Differences in frontal and limbic brain activation in a small sample of monozygotic twin pairs discordant for severe stressful life events. *Neurobiol Stress*, 5:26–36.

Goncharova II, McFarland DJ, Vaughan TM, Wolpaw JR. (2003). EMG contamination of EEG: spectral and topographical characteristics. *Clin Neurophysiol Off J Int Fed Clin Neurophysiol*, 114:1580–1593.

Gramfort A, Luessi M, Larson E, Engemann DA, Strohmeier D, Brodbeck C, Goj R, Jas M, Brooks T, Parkkonen L, Hämäläinen M. (2013). MEG and EEG data analysis with MNE-Python. *Front Neurosci*, 7:267.

Gramfort A, Luessi M, Larson E, Engemann DA, Strohmeier D, Brodbeck C, Parkkonen L, Hämäläinen MS. (2014). MNE software for processing MEG and EEG data. *NeuroImage*, 86:446–460.

Grassi G, Pisano A, Bolignano D, Seravalle G, D'Arrigo G, Quarti-Trevano F, Mallamaci F, Zoccali C, Mancia G. (2018). Sympathetic Nerve Traffic Activation in Essential Hypertension and Its Correlates: Systematic Reviews and Meta-Analyses. *Hypertens Dallas Tex 1979*, 72:483–491.

Guyenet PG. (2006). The sympathetic control of blood pressure. *Nat Rev Neurosci*, 7:335–346.

Guyenet PG, Schreihofer AM, Stornetta RL. (2001). Regulation of sympathetic tone and arterial pressure by the rostral ventrolateral medulla after depletion of C1 cells in rats. *Ann N Y Acad Sci*, 940:259–269.

Guyton AC, Coleman TG, Fourcade JC, Navar LG. (1969). Physiologic control of arterial pressure.. *Bull N Y Acad Med*, 45:811–830.

Hagbarth KE, Vallbo AB. (1968). Pulse and respiratory grouping of sympathetic impulses in human muscle-nerves. *Acta Physiol Scand*, 74:96–108.

Henry JP, Liu YY, Nadra WE, Qian CG, Mormede P, Lemaire V, Ely D, Hendley ED. (1993). Psychosocial stress can induce chronic hypertension in normotensive strains of rats. *Hypertens Dallas Tex 1979*, 21:714–723.

Hollenberg NK, Martinez G, McCullough M, Meinking T, Passan D, Preston M, Rivera A, Taplin D, Vicaria-Clement M. (1997). Aging, acculturation, salt intake, and hypertension in the Kuna of Panama. *Hypertens Dallas Tex 1979*, 29:171–176.

Horiuchi J, Atik A, Iigaya K, McDowall LM, Killinger S, Dampney RAL. (2011). Activation of 5-hydroxytryptamine-1A receptors suppresses cardiovascular responses evoked from the paraventricular nucleus. *Am J Physiol Regul Integr Comp Physiol*, 301:R1088-1097.

Hornyak M, Cejnar M, Elam M, Matousek M, Wallin BG. (1991). Sympathetic muscle nerve activity during sleep in man. *Brain J Neurol*, 114 (Pt 3):1281–1295.

Ito H, Nagano M, Suzuki H, Murakoshi T. (2010). Chronic stress enhances synaptic plasticity due to disinhibition in the anterior cingulate cortex and induces hyper-locomotion in mice. *Neuropharmacology*, 58:746–757.

Ito R, Nakano T, Hojo Y, Hashizume M, Koshiba M, Murakoshi T. (2020). Chronic Restraint Stress Affects Network Oscillations in the Anterior Cingulate Cortex in Mice. *Neuroscience*, 437:172–183.

Jänig W, Häbler H-J. (2003). Neurophysiological analysis of target-related sympathetic pathways – from animal to human: similarities and differences*. *Acta Physiol Scand*, 177:255–274.

Jänig W. (2006). Anatomy of central autonomic systems. In: . *The Integrative Action of the Autonomic Nervous System: Neurobiology of Homeostasis*, . Cambridge University Press.

Jasper H. (1958). Report of the committee on methods of clinical examination in electroencephalography: 1957. *Electroencephalogr Clin Neurophysiol*, 10:370–375.

Joyner MJ, Wallin BG, Charkoudian N. (2016). Sex differences and blood pressure regulation in humans. *Exp Physiol*, 101:349–355.

Kendler KS, Karkowski LM, Prescott CA. (1999). Causal relationship between stressful life events and the onset of major depression. *Am J Psychiatry*, 156:837–841.

Keren AS, Yuval-Greenberg S, Deouell LY. (2010). Saccadic spike potentials in gamma-band EEG: characterization, detection and suppression. *NeuroImage*, 49:2248–2263.

Kilavik BE, Zaepffel M, Brovelli A, MacKay WA, Riehle A. (2013). The ups and downs of β oscillations in sensorimotor cortex. *Exp Neurol*, 245:15–26.

Korner P. (2007). Essential Hypertension and its Causes - Neural and Non-neural mechanisms. New York, NY: Oxford University Press.

Kozlowska K, Walker P, McLean L, Carrive P. (2015). Fear and the Defense Cascade: Clinical Implications and Management. *Harv Rev Psychiatry*, 23:263–287.

Lawler JE, Barker GF, Hubbard JW, Cox RH, Randall GW. (1984). Blood pressure and plasma renin activity responses to chronic stress in the borderline hypertensive rat. *Physiol Behav*, 32:101–105.

Lederbogen F, Kirsch P, Haddad L, Streit F, Tost H, Schuch P, Wust S, Pruessner JC, Rietschel M, Deuschle M, Meyer-Lindenberg A. (2011). City living and urban upbringing affect neural social stress processing in humans. *Nature*, 474:498–501.

LeDoux J, Daw ND. (2018). Surviving threats: neural circuit and computational implications of a new taxonomy of defensive behaviour. *Nat Rev Neurosci*, 19:269–282.

Li SG, Lawler JE, Randall DC, Brown DR. (1997). Sympathetic nervous activity and arterial pressure responses during rest and acute behavioral stress in SHR versus WKY rats. *J Auton Nerv Syst*, 62:147–154.

Lim SS, Vos T, Flaxman AD, Danaei G, Shibuya K, Adair-Rohani H, Amann M, Anderson HR, Andrews KG, Aryee M, Atkinson C, Bacchus LJ, Bahalim AN, Balakrishnan K, Balmes J, Barker-Collo S, Baxter A, Bell ML, Blore JD, Blyth F, Bonner C, Borges G, Bourne R, Boussinesq M, Brauer M, Brooks P, Bruce NG, Brunekreef B, Bryan-Hancock C, Bucello C, Buchbinder R, Bull F, Burnett RT, Byers TE, Calabria B, Carapetis J, Carnahan E, Chafe Z, Charlson F, Chen H, Chen JS, Cheng AT-A, Child JC, Cohen A, Colson KE, Cowie BC, Darby S, Darling S, Davis A, Degenhardt L, Dentener F,

Des Jarlais DC, Devries K, Dherani M, Ding EL, Dorsey ER, Driscoll T, Edmond K, Ali SE, Engell RE, Erwin PJ, Fahimi S, Falder G, Farzadfar F, Ferrari A, Finucane MM, Flaxman S, Fowkes FGR, Freedman G, Freeman MK, Gakidou E, Ghosh S, Giovannucci E, Gmel G, Graham K, Grainger R, Grant B, Gunnell D, Gutierrez HR, Hall W, Hoek HW, Hogan A, Hosgood HD, Hoy D, Hu H, Hubbell BJ, Hutchings SJ, Ibeanusi SE, Jacklyn GL, Jasrasaria R, Jonas JB, Kan H, Kanis JA, Kassebaum N, Kawakami N, Khang Y-H, Khatibzadeh S, Khoo J-P, Kok C, Laden F, Lalloo R, Lan Q, Lathlean T, Leasher JL, Leigh J, Li Y, Lin JK, Lipshultz SE, London S, Lozano R, Lu Y, Mak J, Malekzadeh R, Mallinger L, Marcenes W, March L, Marks R, Martin R, McGale P, McGrath J, Mehta S, Mensah GA, Merriman TR, Micha R, Michaud C, Mishra V, Mohd Hanafiah K, Mokdad AA, Morawska L, Mozaffarian D, Murphy T, Naghavi M, Neal B, Nelson PK, Nolla JM, Norman R, Olives C, Omer SB, Orchard J, Osborne R, Ostro B, Page A, Pandey KD, Parry CDH, Passmore E, Patra J, Pearce N, Pelizzari PM, Petzold M, Phillips MR, Pope D, Pope CA, Powles J, Rao M, Razavi H, Rehfuess EA, Rehm JT, Ritz B, Rivara FP, Roberts T, Robinson C, Rodriguez-Portales JA, Romieu I, Room R, Rosenfeld LC, Roy A, Rushton L, Salomon JA, Sampson U, Sanchez-Riera L, Sanman E, Sapkota A, Seedat S, Shi P, Shield K, Shivakoti R, Singh GM, Sleet DA, Smith E, Smith KR, Stapelberg NJC, Steenland K, Stöckl H, Stovner LJ, Straif K, Straney L, Thurston GD, Tran JH, Van Dingenen R, van Donkelaar A, Veerman JL, Vijayakumar L, Weintraub R, Weissman MM, White RA, Whiteford H, Wiersma ST, Wilkinson JD, Williams HC, Williams W, Wilson N, Woolf AD, Yip P, Zielinski JM, Lopez AD, Murray CJL, Ezzati M, AlMazroa MA, Memish ZA. (2012). A comparative risk assessment of burden of disease and injury attributable to 67 risk factors and risk factor clusters in 21 regions, 1990-2010: a systematic analysis for the Global Burden of Disease Study 2010. *Lancet Lond Engl*, 380:2224–2260.

Liu Q, Liu A, Zhang X, Chen X, Qian R, Chen X. (2019). Removal of EMG Artifacts from Multichannel EEG Signals Using Combined Singular Spectrum Analysis and Canonical Correlation Analysis. *J Healthc Eng*, 2019:4159676.

Lopes da Silva F. (2010). Electrophysiological basis of MEG signals. In: Hansen, PC, Kringelbach, M, Salmelin, R, editors.. *MEG: an introduction to methods*, . New York, NY: Oxford University Press.

Low DA, Keller DM, Wingo JE, Brothers RM, Crandall CG. (2011). Sympathetic nerve activity and whole body heat stress in humans. *J Appl Physiol Bethesda Md 1985*, 111:1329–1334.

Lundblad LC, Eskelin JJ, Karlsson T, Wallin BG, Elam M. (2017). Sympathetic Nerve Activity in Monozygotic Twins: Identical at Rest but Not During Arousal. *Hypertens Dallas Tex 1979*, 69:964–969.

Macefield VG, Rundqvist B, Sverrisdottir YB, Wallin BG, Elam M. (1999). Firing properties of single muscle vasoconstrictor neurons in the sympathoexcitation associated with congestive heart failure. *Circulation*, 100:1708–1713.

Macefield VG, Wallin BG. (2018). Physiological and pathophysiological firing properties of single postganglionic sympathetic neurons in humans. *J Neurophysiol*, 119:944–956.

Maguire EA, Gadian DG, Johnsrude IS, Good CD, Ashburner J, Frackowiak RS, Frith CD. (2000). Navigation-related structural change in the hippocampi of taxi drivers. *Proc Natl Acad Sci U A*, 97:4398–403.

Maris E, Oostenveld R. (2007). Nonparametric statistical testing of EEG- and MEG-data. *J Neurosci Methods*, 164:177–190.

Mark AL, Victor RG, Nerhed C, Wallin BG. (1985). Microneurographic studies of the mechanisms of sympathetic nerve responses to static exercise in humans. *Circ Res*, 57:461–469.

McAllen RM, Malpas SC. (1997). Sympathetic burst activity: characteristics and significance. *Clin Exp Pharmacol Physiol*, 24:791–799.

McMenamin BW, Shackman AJ, Greischar LL, Davidson RJ. (2011). Electromyogenic Artifacts and Electroencephalographic Inferences Revisited. *NeuroImage*, 54:4–9.

Merkl A, Neumann W-J, Huebl J, Aust S, Horn A, Krauss JK, Dziobek I, Kuhn J, Schneider G-H, Bajbouj M, Kühn AA. (2016). Modulation of Beta-Band Activity in the Subgenual Anterior Cingulate Cortex during Emotional Empathy in Treatment-Resistant Depression. *Cereb Cortex N Y N 1991*, 26:2626–2638.

Muthukumaraswamy SD, Myers JFM, Wilson SJ, Nutt DJ, Lingford-Hughes A, Singh KD, Hamandi K. (2013). The effects of elevated

endogenous GABA levels on movement-related network oscillations. *NeuroImage*, 66:36–41.

Muthukumaraswamy SD. (2013). High-frequency brain activity and muscle artifacts in MEG/EEG: a review and recommendations. *Front Hum Neurosci*, 7:138.

NCD-RisC. (2017). Worldwide trends in blood pressure from 1975 to 2015: a pooled analysis of 1479 population-based measurement studies with 19·1 million participants. *Lancet Lond Engl*, 389:37–55.

Ng AV, Callister R, Johnson DG, Seals DR. (1993). Age and gender influence muscle sympathetic nerve activity at rest in healthy humans. *Hypertens Dallas Tex 1979*, 21:498–503.

Olbrich S, Jödicke J, Sander C, Himmerich H, Hegerl U. (2011). ICA-based muscle artefact correction of EEG data: what is muscle and what is brain? Comment on McMenamin et al. *NeuroImage*, 54:1–3; discussion 4-9.

Oostenveld R, Fries P, Maris E, Schoffelen J-M. (2011). FieldTrip: Open source software for advanced analysis of MEG, EEG, and invasive electrophysiological data. *Comput Intell Neurosci*, 2011:156869.

Oppenheimer SM, Gelb A, Girvin JP, Hachinski VC. (1992). Cardiovascular effects of human insular cortex stimulation. *Neurology*, 42:1727–1727.

Oppenheimer SM, Wilson JX, Guiraudon C, Cechetto DF. (1991). Insular cortex stimulation produces lethal cardiac arrhythmias: a mechanism of sudden death?. *Brain Res*, 550:115–121.

Palomero-Gallagher N, Vogt BA, Schleicher A, Mayberg HS, Zilles K. (2009). Receptor architecture of human cingulate cortex: evaluation of the four-region neurobiological model. *Hum Brain Mapp*, 30:2336–55.

Parkkonen L. (2010). Instrumentaion and data processing. In: Hansen, PC, Kringelbach, M, Salmelin, R, editors.. *MEG: an introduction to methods*, . New York, NY: Oxford University Press.

Pfeiffer C, Ruffieux S, Jönsson L, Chukharkin ML, Kalaboukhov A, Xie M, Winkler D, Schneiderman JF. (2020). A 7-Channel High-Tc SQUID-Based On-Scalp MEG System. *IEEE Trans Biomed Eng*, 67:1483–1489.

Posch AM, Luippold AJ, Mitchell KM, Bradbury KE, Kenefick RW, Cheuvront SN, Charkoudian N. (2017). Sympathetic neural and

hemodynamic responses to head-up tilt during isoosmotic and hyperosmotic hypovolemia. *J Neurophysiol*, 118:2232–2237.

Puce A, Hämäläinen MS. (2017). A Review of Issues Related to Data Acquisition and Analysis in EEG/MEG Studies. *Brain Sci*, 7.

Reckelhoff JF. (2001). Gender differences in the regulation of blood pressure. *Hypertens Dallas Tex 1979*, 37:1199–1208.

Robinson AT, Babcock MC, Watso JC, Brian MS, Migdal KU, Wenner MM, Farquhar WB. (2019). Relation between resting sympathetic outflow and vasoconstrictor responses to sympathetic nerve bursts: sex differences in healthy young adults. *Am J Physiol Regul Integr Comp Physiol*, 316:R463–R471.

Roy M, Shohamy D, Wager TD. (2012). Ventromedial prefrontal-subcortical systems and the generation of affective meaning. *Trends Cogn Sci*, 16:147–156.

Salenius S, Schnitzler A, Salmelin R, Jousmäki V, Hari R. (1997). Modulation of human cortical rolandic rhythms during natural sensorimotor tasks. *Neuroimage*, 5:221–228.

Scalco AZ, Rondon MUPB, Trombetta IC, Laterza MC, Azul JBCC, Pullenayegum EM, Scalco MZ, Kuniyoshi FHS, Wajngarten M, Negrão CE, Lotufo-Neto F. (2009). Muscle sympathetic nervous activity in depressed patients before and after treatment with sertraline. *J Hypertens*, 27:2429–2436.

Schreihofer AM, Guyenet PG. (2002). The baroreflex and beyond: control of sympathetic vasomotor tone by GABAergic neurons in the ventrolateral medulla. *Clin Exp Pharmacol Physiol*, 29:514–521.

Shackman AJ, McMenamin BW, Slagter HA, Maxwell JS, Greischar LL, Davidson RJ. (2009). Electromyogenic artifacts and electroencephalographic inferences. *Brain Topogr*, 22:7–12.

Shoemaker JK, Klassen SA, Badrov MB, Fadel PJ. (2018). Fifty years of microneurography: learning the language of the peripheral sympathetic nervous system in humans. *J Neurophysiol*, 119:1731–1744.

Sluming V, Barrick T, Howard M, Cezayirli E, Mayes A, Roberts N. (2002). Voxel-based morphometry reveals increased gray matter density in Broca's area in male symphony orchestra musicians. *Neuroimage*, 17:1613–22.

Stevens SL, Wood S, Koshiaris C, Law K, Glasziou P, Stevens RJ, McManus RJ. (2016). Blood pressure variability and cardiovascular disease: systematic review and meta-analysis. *BMJ*, 354:i4098.

Sundlöf G, Wallin BG. (1978). Human muscle nerve sympathetic activity at rest. Relationship to blood pressure and age. *J Physiol*, 274:621–637.

Tank J, Heusser K, Diedrich A, Hering D, Luft FC, Busjahn A, Narkiewicz K, Jordan J. (2008). Influences of gender on the interaction between sympathetic nerve traffic and central adiposity. *J Clin Endocrinol Metab*, 93:4974–4978.

Timio M, Lippi G, Venanzi S, Gentili S, Quintaliani G, Verdura C, Monarca C, Saronio P, Timio F. (1997). Blood pressure trend and cardiovascular events in nuns in a secluded order: a 30-year follow-up study. *Blood Press*, 6:81–87.

Timio M, Saronio P, Venanzi S, Gentili S, Verdura C, Timio F. (1999). Blood pressure in nuns in a secluded order: A 30-year follow-up. *Miner Electrolyte Metab*, 25:73–79.

Timio M, Verdecchia P, Venanzi S, Gentili S, Ronconi M, Francucci B, Montanari M, Bichisao E. (1988). Age and blood pressure changes. A 20-year follow-up study in nuns in a secluded order. *Hypertens Dallas Tex 1979*, 12:457–461.

Vallbo AB, Hagbarth KE, Torebjörk HE, Wallin BG. (1979). Somatosensory, proprioceptive, and sympathetic activity in human peripheral nerves. *Physiol Rev*, 59:919–957.

Victor RG, Leimbach WN, Seals DR, Wallin BG, Mark AL. (1987). Effects of the cold pressor test on muscle sympathetic nerve activity in humans. *Hypertens Dallas Tex 1979*, 9:429–436.

Wager TD, Waugh CE, Lindquist M, Noll DC, Fredrickson BL, Taylor SF. (2009). Brain mediators of cardiovascular responses to social threat: part I: Reciprocal dorsal and ventral sub-regions of the medial prefrontal cortex and heart-rate reactivity. *NeuroImage*, 47:821–835.

Wallin BG, Elam M. (1997). Cutaneous Sympathetic Nerve Activity in Humans. In: Morris, JL, Gibbins, IL, editors.. *Autonomic Innervation of the Skin*, . Netherlands: Harwood Academic Publishers. The Autonomic Nervous System.

Wallin BG, Kunimoto MM, Sellgren J. (1993). Possible genetic influence on the strength of human muscle nerve sympathetic activity at rest. *Hypertension*, 22:282–4.

Wallin BG, Nerhed C. (1982). Relationship between spontaneous variations of muscle sympathetic activity and succeeding changes of blood pressure in man. *J Auton Nerv Syst*, 6:293–302.

Wallin BG, Rea R. (1988). Spinal sympathetic conduction velocity in humans. *J Auton Nerv Syst*, 24:221–225.

Wallin BG. (1988). Relationship Between Sympathetic Nerve Traffic and Plasma Concentrations of Noradrenaline in Man. *Pharmacol Toxicol*, 63:9–11.

Wallin BG. (2006). Regulation of sympathetic nerve traffic to skeletal muscle in resting humans. *Clin Auton Res Off J Clin Auton Res Soc*, 16:262–269.

Whelton Paul K., Carey Robert M., Aronow Wilbert S., Casey Donald E., Collins Karen J., Dennison Himmelfarb Cheryl, DePalma Sondra M., Gidding Samuel, Jamerson Kenneth A., Jones Daniel W., MacLaughlin Eric J., Muntner Paul, Ovbiagele Bruce, Smith Sidney C., Spencer Crystal C., Stafford Randall S., Taler Sandra J., Thomas Randal J., Williams Kim A., Williamson Jeff D., Wright Jackson T. (2018). 2017 ACC/AHA/AAPA/ABC/ACPM/AGS/APhA/ASH/ASPC/NMA/PCNA Guideline for the Prevention, Detection, Evaluation, and Management of High Blood Pressure in Adults: Executive Summary: A Report of the American College of Cardiology/American Heart Association Task Force on Clinical Practice Guidelines. *Hypertension*, 71:1269–1324.

Whitham EM, Lewis T, Pope KJ, Fitzgibbon SP, Clark CR, Loveless S, DeLosAngeles D, Wallace AK, Broberg M, Willoughby JO. (2008). Thinking activates EMG in scalp electrical recordings. *Clin Neurophysiol Off J Int Fed Clin Neurophysiol*, 119:1166–1175.

Whitham EM, Pope KJ, Fitzgibbon SP, Lewis T, Clark CR, Loveless S, Broberg M, Wallace A, DeLosAngeles D, Lillie P, Hardy A, Fronsko R, Pulbrook A, Willoughby JO. (2007). Scalp electrical recording during paralysis: quantitative evidence that EEG frequencies above 20 Hz are contaminated by EMG. *Clin Neurophysiol Off J Int Fed Clin Neurophysiol*, 118:1877–1888.

Yamada Y, Miyajima E, Tochikubo O, Matsukawa T, Ishii M. (1989). Age-related changes in muscle sympathetic nerve activity in essential hypertension. *Hypertens Dallas Tex 1979*, 13:870–877.

Yao D, Qin Y, Hu S, Dong L, Bringas Vega ML, Valdés Sosa PA. (2019). Which Reference Should We Use for EEG and ERP practice?. *Brain Topogr*, 32:530–549.

Yao D, Wang L, Oostenveld R, Nielsen KD, Arendt-Nielsen L, Chen ACN. (2005). A comparative study of different references for EEG spectral mapping: the issue of the neutral reference and the use of the infinity reference. *Physiol Meas*, 26:173–184.

Yilmaz G, Ungan P, Sebik O, Uginčius P, Türker KS. (2014). Interference of tonic muscle activity on the EEG: a single motor unit study. *Front Hum Neurosci*, 8. https://www.ncbi.nlm.nih.gov/pmc/articles/PMC4092367/.